DEVELOPMENT OF A CONTROLLER FOR FUEL CELL USING FPGA

A thesis submitted in partial fulfilment of the requirements for the degree of

Master of Technology
in
VLSI Design & Embedded System
by

Sadhana Kumari

Roll No. 209ec2129

Under the guidance of
Prof. Kamalakanta Mahapatra

Department of Electronics & Communication Engineering
National Institute of Technology, Rourkela, Odisha

2011

National Institute of Technology Rourkela

CERTIFICATE

This is to certify that the thesis entitled, "**DEVELOPMENT OF A CONTROLLER FOR FUEL CELL USING FPGA**" submitted by SADHANA KUMARI (Roll No.-209ec2129) in partial fulfilment of the requirements for the degree of Master of Technology in VLSI Design & Embedded system, Session 2009-2011, in the Department of Electronics and Communication Engineering, National Institute of Technology, Rourkela is an authentic work carried out by her under my supervision and guidance.

To the best of my knowledge, the matter embodied in the thesis has not been submitted to any other University / Institute for the award of any Degree.

Date:

Prof. K.K.Mahapatra
SUPERVISOR
Dept. of Electronics & Communication Engineering
National Institute of Technology Rourkela –769008

National Institute Of Technology
Rourkela

DECLARATION

I hereby declare that this thesis entitled **"DEVELOPMENT OF A CONTROLLER FOR FUEL CELL USING FPGA"** submitted to National Institute of Technology, Rourkela for the award of the degree of Master of Technology is a record of original work done by me under the guidance Prof. Kamalakanta Mahapatra and that it has not been used, they have been acknowledged.

Place: ROURKELA

Date: Signature

ACKNOWLEDGEMENTS

I am heartily thankful to my supervisor, **Prof. Kamalakanta Mahapatra**, whose encouragement, guidance and support from the initial to the final level enabled me to develop an understanding of the concept, which was very necessary for me. He had been very kind and patient while suggesting me the topics and correcting my doubts.

I am equally grateful to Mr.P.Karupanan (Ph.D Scholar), and Mr. Ayashkant Swain, Lab Engineer for their positive support, despite of their busy schedule, they gave me different ideas in making this project unique.

Last but certainly not the least; I would like to show my gratitude to my parents and my friends that had a positive influence in my life.

Lastly, I offer my regards and best wishes to all of those who supported me in any respect during the completion of this project.

Thanking you all.

SADHANA KUMARI

Contents *Page no.*

List of figures

List of tables

List of graphs

Abstract

This thesis is a sample of what we can do to reduce the complexity of a fuel cell controller and research carried out in the modeling of a renewable energy sources like fuel cell. This thesis mainly deals the control of the fuel cell under variation of different parameters, and implementation of the system in VHDL. As we know that not any voltage source, weather it is traditional energy source or fuel cell system behaves as an ideal source. The output of these cells depends upon some parameter of the cell. To control the output voltage of a fuel cell we need some controller, it may be digital or analog.

At the present time, PWM has become an integral part of all the electronic system. This technique has some salient feature, due to which it has replaced the traditional use of digitally just on off signal to control the switching action of the converter. There are two basic techniques of PWM generation, analog and digital. The disadvantages of the analog methods are that they are prone to noise, and they change with voltage and temperature change, they suffer changes due to component variation. To overcome the problem, associated with the analog technique, various types of digital technique are available. Implementation of these techniques in VHDL has done.

First we have synthesized the whole system, using Matlab/Simulink then VHDL code for various topology of digital technique of PWM generation. After behavioral Simulation and verification of the results this VHDL code has downloaded to SPARTAN3E FPGA. After downloading the code in FPGA real time debugging has done for the architecture. The overall work done in this thesis aims to promote professional activity in the area of fuel cell controller and low power electronics used in the modern age, with an important focus on the design, development, simulation, and verification, and to examine the possibility of using Field Programmable Gate Arrays (FPGA) for the rapid prototyping of a PI+PWM digital electronic controller used in a power system consisting of a 2.4 kW 96 v fuel cell system, which is made up of two main component, fuel cell stack and boost converter.

***Key terms*: PWM, Boost Converter, FPGA, PEM fuel cell**.

Chapter 1

Introduction

Chapter1

Introduction

Now this is the age of VLSI and this technology has become advanced and more prominent, due to development of EDA tools. To design a Novel system often means that the design should reach certain goal under certain constraint applied to it, and to perform better in the operating limit for which the system has to be design. Holistic modelling of any complex system plays the vital role in the design of the system. The goal of this thesis is to examine the possibility of FPGA based hardware prototyping for a complex fuel cell system, so that we can use this system controller efficiently for controlling the voltage. Traditional methods are not able to cope with increased complexity and demand of very higher level of system integration and relatively short time to market. Nowadays functional description and hardware implementation has brought to be closer with the help of recent advancement in CAD methodologies/language. The chief contribution of this work is to demonstrate control techniques based on system level digital language, which can show the possibility of using an FPGA based digital controller to reduce the system complexity, and also increase its reusability.

1.1 Advantage of modeling of fuel cell

Successful innovation often means a design that achieves a desirable cluster of performance characteristics, subject to certain constrains and holistic modelling of complex technical systems can constitute the first step towards novel designs of high performance [1]. FCS (fuel cell system) is a good energy sources to provide reliable power at steady state; however, due to their slow internal electrochemical and thermodynamic characteristics, they cannot respond to electrical load transients as quickly as desired. They are connected to the power grid through power electronic interfacing devices, and it is possible to control their performance by controlling the interfacing devices. Modeling of FCS can therefore be helpful in evaluating their performance and for designing controllers [2]. Modelling of any complex system gives a mathematical description and provides a way to implement the whole system on a single platform. Holistic modelling of complex technical systems can constitute the first step towards the creation of novel circuit designs of high performance [3]. A holistic, system level, approach to the design and development of an electronic system enables a top-down

design methodology, which begins with modelling an idea at an abstract level, and proceeds through the iterative steps necessary to further refine this into a detailed system [3].

1.2 Advantages of FPGA based design

Field programmable gate array are a special class of ASIC'S. Advantages offered by FPGA are [4].

- Cost .reduction
- Confidentiality.
- Embedded system.
- Improvement of control performance.

Fuel cell output voltage depends upon various design parameters, and it is a unique function of these parameters. To design a controller for this energy source is a complex problem. This problem can be short out with the help of prototyping and behavioural synthesis of the controller on the FPGA.

1.3 PWM Technique

A modulation technique that generates variable width pulses to represent the amplitude of an analog input signal. Pulse Width Modulation (PWM) has now become an integral part of almost all embedded systems. It has been widely accepted as control technique in most of the electronic appliances. Pulse width modulation (PWM) is a powerful technique for controlling analog circuits with a processor's digital outputs. PWM is employed in a wide variety of applications, ranging from measurement and communications to power control and conversion. There are various methods depending upon architecture and requirement of the system. Their design implementation depends upon application type, power consumption, semiconductor devices, performance and cost criteria, these all determine the PWM method [5]. Digital methods are the most suited form for designing PWM generators, because they are very flexible and less sensitive to environmental noise [5].

1.4 Fuel Cell system Implementation in system level language

This thesis describes holistic modelling of the fuel cell different techniques of the voltage converter, and different techniques of digital controller design, and hardware prototyping of a 2.4 kW fuel cell energy system for supplying a 96v dc voltage load. There are certain advantages of this thesis, such as: the modelling of fuel cell, parameter evaluation of fuel cell hardware prototyping of the digital controller (PI+PWM).

The experimental validation has done, by taking Simulink of fuel cell system as reference. A fuel cell system has developed in VHDL which allows FPGA based prototyping for controller part, after that, experimental validation has done through comparison between the reference (MATLAB/Simulink) and VHDL implemented system.

Chapter 2

An Introduction to the Fuel Cell and its Modeling

Chapter 2

An Introduction to the Fuel cell and its Modeling

2.1 Introduction

A fuel cell is a device that converts the chemical energy of a fuel and an oxidant directly into electricity. Operating principal of fuel cell is almost similar to that of the battery, but unlike a battery a fuel cell is a renewable source of energy, which runs continuously, if we supply fuel and an oxidant to it.

In a fuel cell, the same basic chemical reactions, as occur in traditional method of generation of heat, but generate electricity directly as an electrochemical device. This direct conversion of chemical energy to electrical energy is more efficient and generates much less pollutants than traditional methods that based on combustion of reactants.

The basic physical structure or building block of a fuel cell consists of an electrolyte layer in contact with a porous anode and cathode on either side. A schematic representation of a fuel cell with the reactant/product gases and the ion conduction flow directions through the cell is shown in Fig. 2.1.

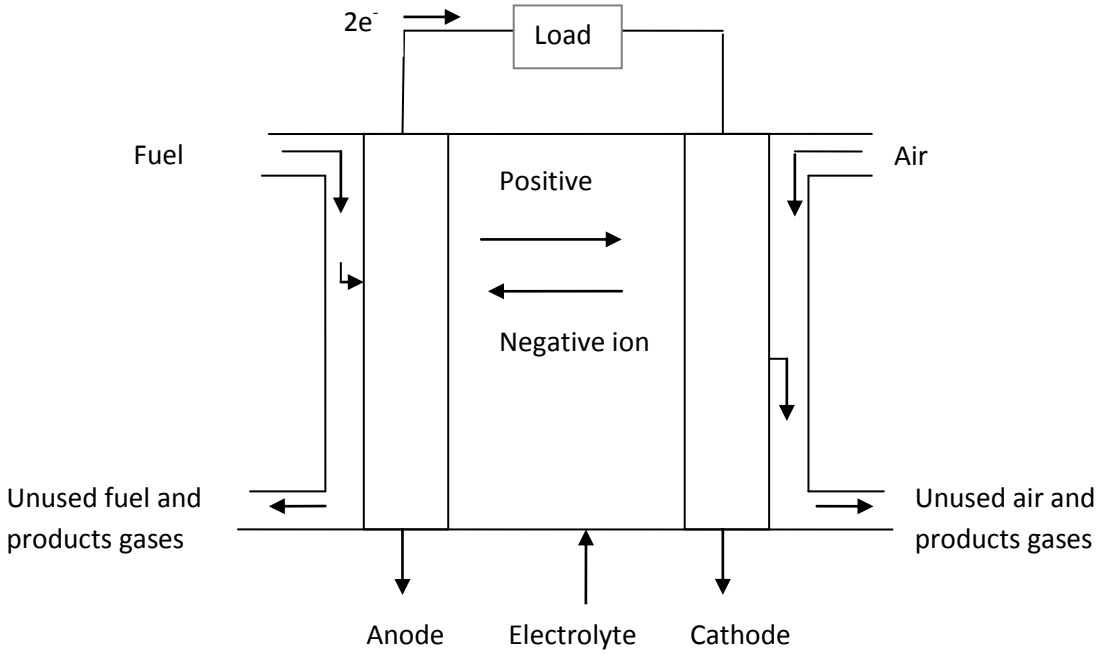

Fig.2.1 Schematic of Fuel Cell

There are different technologies of fuel cell. They are commonly classified according to their operating temperature and/or the type of electrolyte. Due to certain advantages (high

efficiency, low operating temperature) of PEM (polymer electrolyte membrane) fuel cell, over other fuel cell, nowadays people prefer PEMFC to other conventional type fuel cell. Polymer electrolyte membrane (PEM) fuel cells are the most popular type of fuel cell, and traditionally use hydrogen as the fuel. PEM fuel cells also have many other fuel options, which range from hydrogen to ethanol to biomass-derived materials. These fuels can either be directly fed into the fuel cell, or sent to a reformer to extract pure hydrogen, which is then directly fed to the fuel cell [5].

2.2 PEMFC Functionality

Fuel cells generate electricity from a simple electrochemical reaction in which an oxidizer, typically oxygen from air, and a fuel, typically hydrogen, combine to form a product, which is water for the typical fuel cell. Oxygen (air) continuously passes over the cathode, and hydrogen passes over the anode to generate electricity, by-product heat and water. As the name suggests, in between the anode and cathode terminals, there is a membrane (electrolyte) can conduct only positive charge ion. Sulphonated polymer (NAFLON) can be used as a membrane of the PEMFC.

The reactions are shown below.

Reaction at Anode:

$$2H_2 \rightarrow 4H^+ + 4e^- \quad (1)$$

Reaction at Cathode**:**

$$O_2 + 4H^+ + 4e^- \rightarrow 2H_2O \quad (2)$$

The electron freed at anode travels through another wire and react with the oxygen as well as proton thus water is produced. When the electron travels through external circuit, electricity is also produced.

Cathode and anode both have channel etched into it, which disperse the H_2 gas equally over the surface of the catalyst. Individual fuel cells can then be combined into a fuel cell stack to take a desired power from the fuel cell. The number of fuel cells in the stack determines the total voltage taken from the stack of fuel cell, and the surface area of each cell determines the total current.

Modeling of PEMFC:

To achieve desirable performance characteristics, under certain constraints, Holistic modeling of complex technical systems can constitute the first step. The model of fuel cell separated in two parts as denoted in Fig.2.2 [6]:

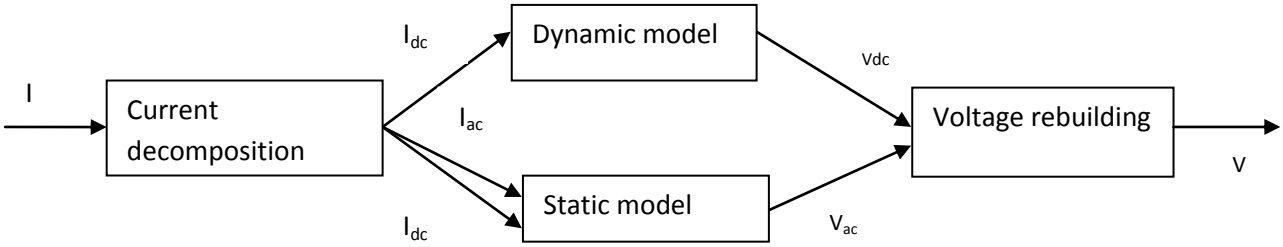

Fig.2.2 Fuel Cell Model

- **Static Model:**

The static model describes the static behaviour of fuel cell, i.e. the value of static fuel cell voltage as a function of the static current of the fuel cell.

- **Dynamic Model:**

The dynamic model based on the small variation of the cell voltage as a result of small current variation. The model is valid only for the small variation of current around a fixed steady point; this is based on the assumption that the fuel cell is a linear system for small signal variation in current.

2.2.1 Static Model

The static model of a fuel cell can be modelled on the basis of the following empirical equation [6].

$$v_{dc} = E_0 - b.\log(a.i_{dc}) - r.i_{dc} - m.\exp(n.i_{dc}) \quad (3)$$

Where; E_0 = current of fuel cell at a current of 0 amp.

i_{dc} = fuel cell static current.

v_{dc}= fuel cell static voltage.

a,b,r,m,n are fuel cell empirical parameters.

2.2.2 Dynamic Model

Fuel Cell Electrochemical Model

Empirical formula for fuel cell voltage is [7]:

$$V_{fc} = E_{cell} - V_{act} - V_{con} - V_{ohmic} \quad (4)$$

Where; E_{cell} is the thermodynamic potential of the cell V_{act} is activation overvoltage, V_{ohmic} is ohmic overvoltage and V_{con} is concentration overvoltage.

I. Nernst voltage (E_{Cell}):

The overall reaction in a PEM fuel cell can be simply written as

$$2H_2 + O_2 \rightarrow 2H_2O \quad (5)$$

The Nernst equation for the hydrogen/oxygen fuel cell for the above reaction is [8]:

$$E_{cell} = E_{0,cell} + \frac{R.T}{2F}.\left[\ln P_{H2} + \frac{1}{2}\ln P_{o2}\right] \quad (6)$$

Where; T is the cell temperature (K), P_{H2} is the partial pressure of hydrogen at the anode catalyst/gas interface (atm), and P_{O2} is the partial pressure of oxygen at the cathode catalyst/gas interface (atm).$E_{0,cell}$ is a function of temperature and can be expressed as [9] :

$$E_{0,cell} = E^{0}{}_{0,cell} - k_E(T - 228) \quad (7)$$

II. Activation loss (V_{act}):

The activation overvoltage is the voltage drop due to the activation of the anode and the cathode. Tafel equation, given below, is used to calculate activation overvoltage in a fuel cell [9]:

$$V_{act} = -\left[\zeta_1 + \zeta_2 T + \zeta_3 T \ln(co_2) + \zeta_4 T \ln\left(i_{Fc}\right)\right] \quad (8)$$

Where; i_{Fc} is cell operating current and *ξ1, ξ2, ξ3 ,ξ4* are parametric coefficient of fuel cell ,C_{o2} is the concentration of dissolved oxygen at liquid gas interface. The value of C_{o2} can be estimated by using [10]:

$$C_{o2} = \frac{P_{o2}}{5.08.10^6 e^{\frac{-498}{T}}} \quad (9)$$

III. Ohmic loss (V_{ohmic})

Ohmic loss of fuel cell using ohm's law is:

$$V_{ohmic} = i_{Fc}.\left(R_{el} + R_{pr}\right) \quad (10)$$

Where; R_{el} is the resistance produced by membrane to electron flow, and R_{Pr} is the resistance to proton flow.

R_{Pr} is usually considered to be constant quantity whereas R_{el} is given by the following equation [11]

$$R_{el} = \rho_m \frac{l}{A} \tag{11}$$

Where; l is membrane thickness (cm), A is the cell active area (cm^2), and ρ_m is specific resistivity of membrane for the electron flow (Ω.cm), which for the Naflon type membrane can be given by [12]:

$$\rho_m = \frac{181.6\left[1 + 0.03.\left(\frac{i_{Fc}}{A}\right) + 0.062 \cdot \left(\frac{T}{303}\right)^2 \cdot \left(\frac{i_{Fc}}{A}\right)^{2.5}\right]}{\left[\psi - 0.634 - 3.\left(\frac{i_{Fc}}{A}\right)\right] \cdot \exp\left(4.18\left(\frac{T-303}{T}\right)\right)} \tag{12}$$

IV. Concentration Voltage Drop:

During the reaction process, concentration gradients can be formed due to mass diffusions from the flow channels to the reaction sites (catalyst surfaces). At high current densities, slow transportation of reactants (products) to (from) the reaction sites is the main reason for the concentration voltage drop [13]. This voltage is given by [1].

$$V_{Con} = -B.\ln\left(1 - \frac{j}{j_{\max}}\right) \tag{13}$$

Where: B represents a parametric coefficient (v), and j represents the actual current density of the cell (A/cm^2) and j_{max} is the limiting current density.

Applying assumption that parameters for individual cells can be lumped together to represent a fuel-cell stack, the output voltage of the fuel-cell stack can be written as [14]:

$$v_{out} = N_{cell}.v_{cell} = N_{cell}(E_{cell} - v_{act} - v_{ohmic} - v_{con}) \tag{14}$$

Where; N_{cell} = Number of fuel cell in stack.

V_{cell} = fuel cell voltage.

E_{cell} = Thermodynamic potential of the fuel cell.

$v_{act}, v_{con}, v_{ohmic}$ are losses, introduced into the fuel cell.

V. Double layer charging effect:

In a PEM fuel cell, the two electrodes are separated by a solid membrane (Fig. 2.1) which only allows the H^+ ions to pass, but prevents the motion of electrons [7],[13]. The electrons at the anode will flow through the external load and comes to the surface of the cathode, to which the protons of hydrogen will be attracted at the same time. Thus, two charged layers of

opposite polarity are formed across the boundary between the porous cathode and the membrane [7], [15]. These two layer separated by the membrane act as double charged layer, which can store electrical energy, due to this property this can be treated as a super capacitor.

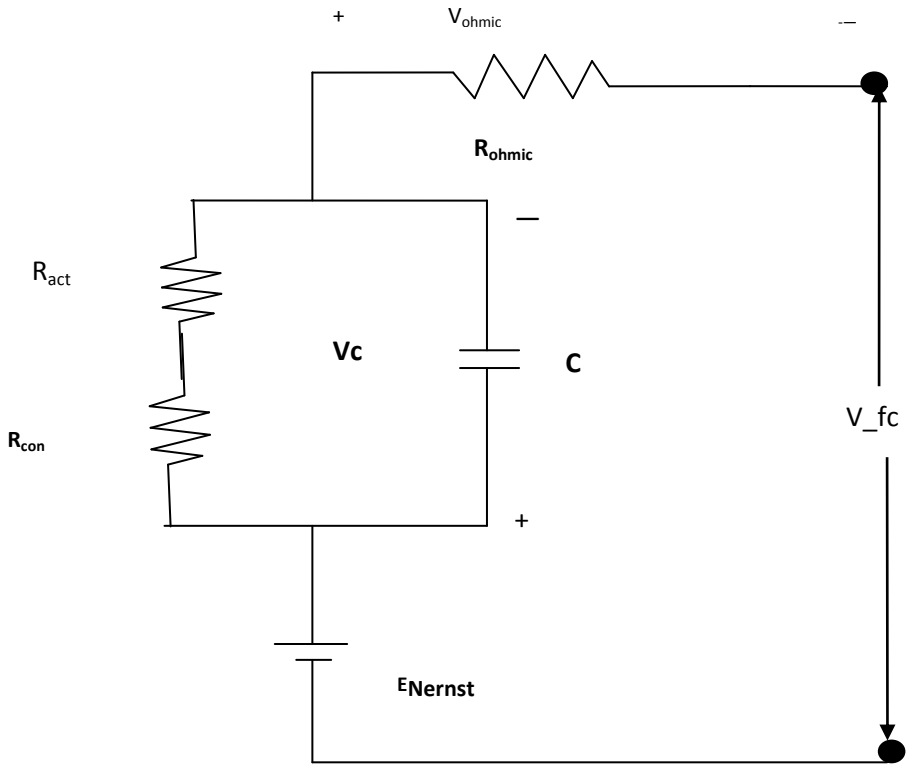

Fig.2.3 Equivalent electrical circuit of PEM fuel cell.

Circuital model of fuel cell by considering all the effect discussed above is shown in Fig.2.3, where the resistances are the equivalent resistance for different types of fuel cell losses.
This model of fuel cell is described by [1]:

$$\frac{dvc}{dt} = \frac{1}{C} i_{Fc} - \frac{1}{\tau} v_c \tag{15}$$

Where v_c is the dynamic voltage of the equivalent electrical capacitance C and τ is the time constant, dependant of the cell temperature given by the equation

$$\tau = c.(R_{act} + R_{con}) \tag{16}$$

We can write (4) as given below

$$v_{Fc} = E_{Nernst} - v_{ohmic} - v_c \tag{17}$$

2.3 MATLAB Simulation Results of all type losses and thermodynamic potential

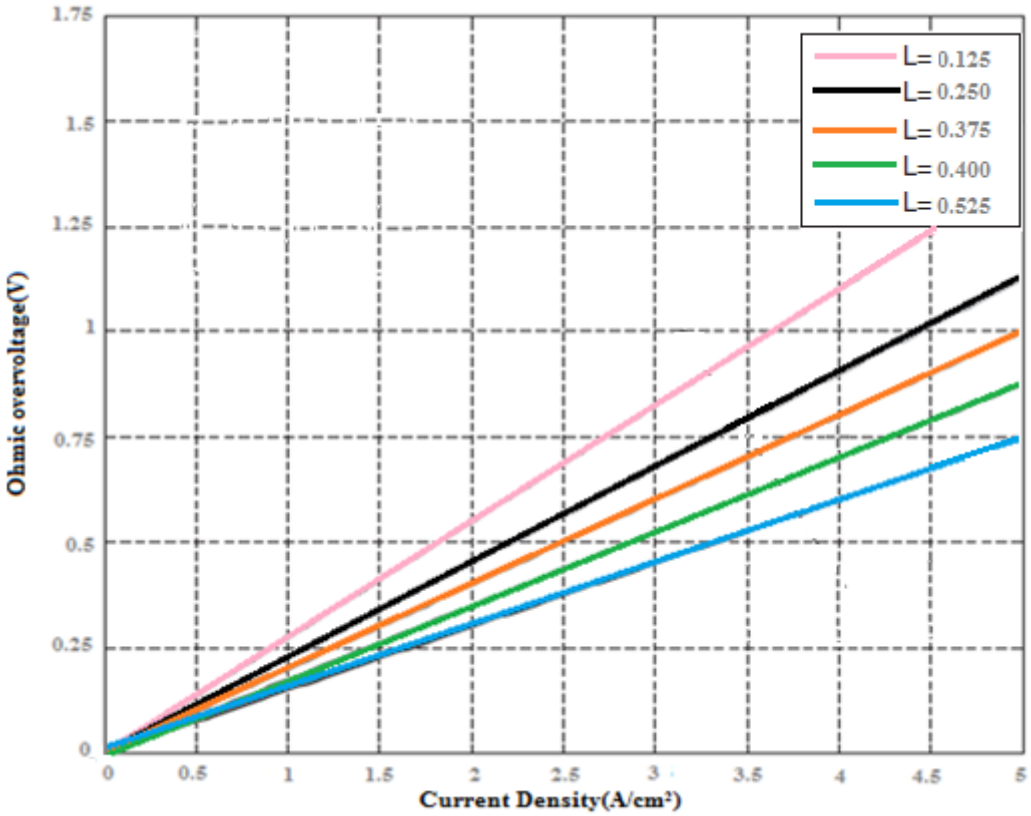

Graph 2.1 Ohmic Loss(function of electrolyte thickness) Versus Current Density

We can see in the above graph, at constant electrolyte thickness ohmic loss is increasing with the increase in the cell current density, and for fixed current density ohmic overvoltage is increasing with the increase in the electrolyte thickness.

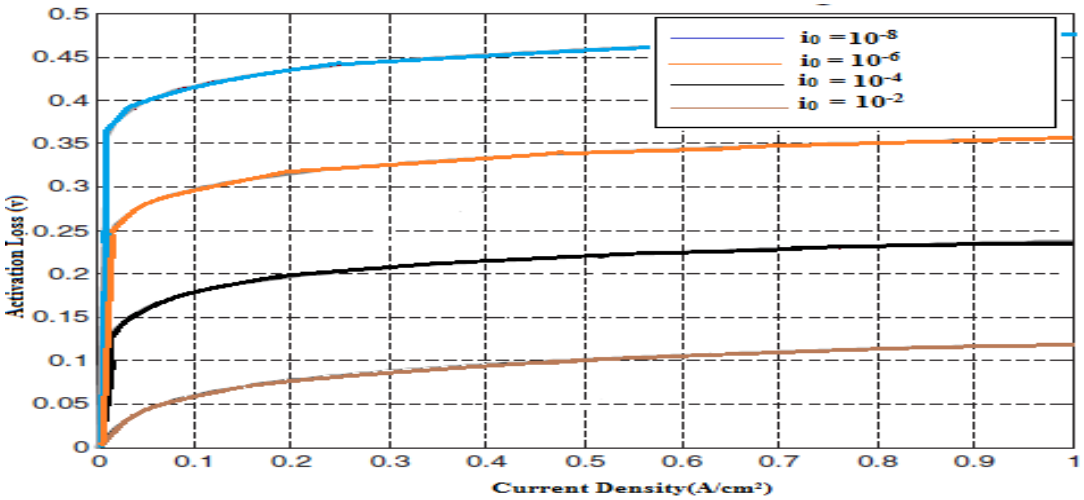

Graph 2.2 Activation Loss (function of limiting current) versus current Density

In the above graph we can see that at a fixed value of limiting current activation loss is increasing with the increase in Cell current density, and at a fixed value of the current density activation loss increasing with increase in limiting current.

If the exchange current is very large, the system will supply large currents with very small activation overvoltage. If a system has an extremely small exchange current density, no significant current will flow unless large activation overpotential is applied.

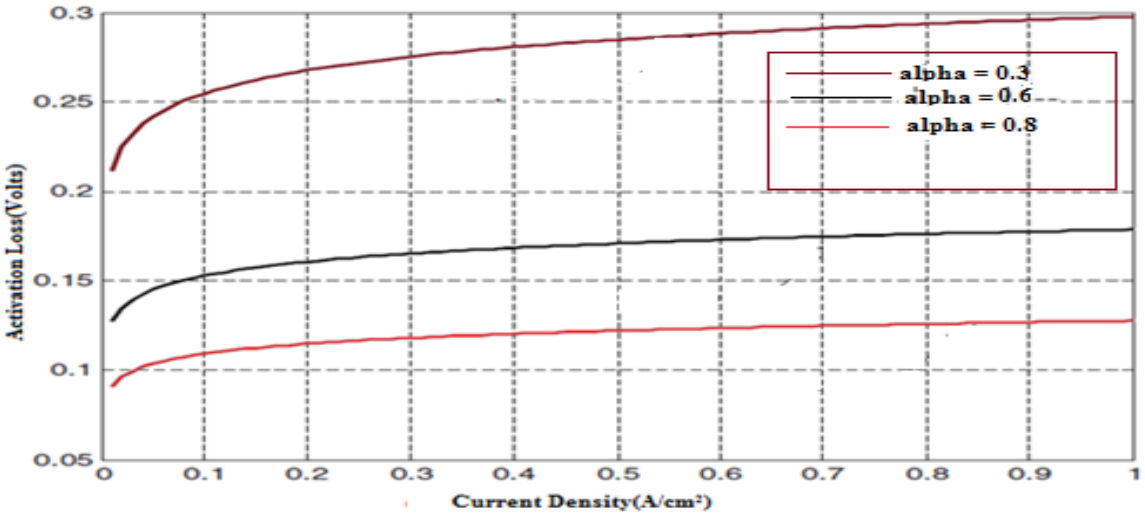

Graph 2.3 Activation Loss(function of transfer coefficient) versus fuel cell current density

Activation loss shown in the above graph (Graph 2.3) is increasing with the increase in the cell current density, however it is decreasing with the increase in the transfer coefficient (denoted as alpha in the graph). In order to simulate the entropy of fuel, water and oxidant, we have taken the value of different parameter, as given in table 2.1.

Table 2.1

Name of parameters	Value
Temperature	353(K)
Reference Temperature	298(K)
Moles of Hydrogen	2.016
Moles of oxygen	31.999
Enthalpy of O2 at standard state	0
Enthalpy of H2 at standard state	0
Moles of H_2O	18
Enthalpy at standard state of water in liquid phase(J/mol)	-285 826
Enthalpy at standard state of water in gas phase(J/mol)	-241 826

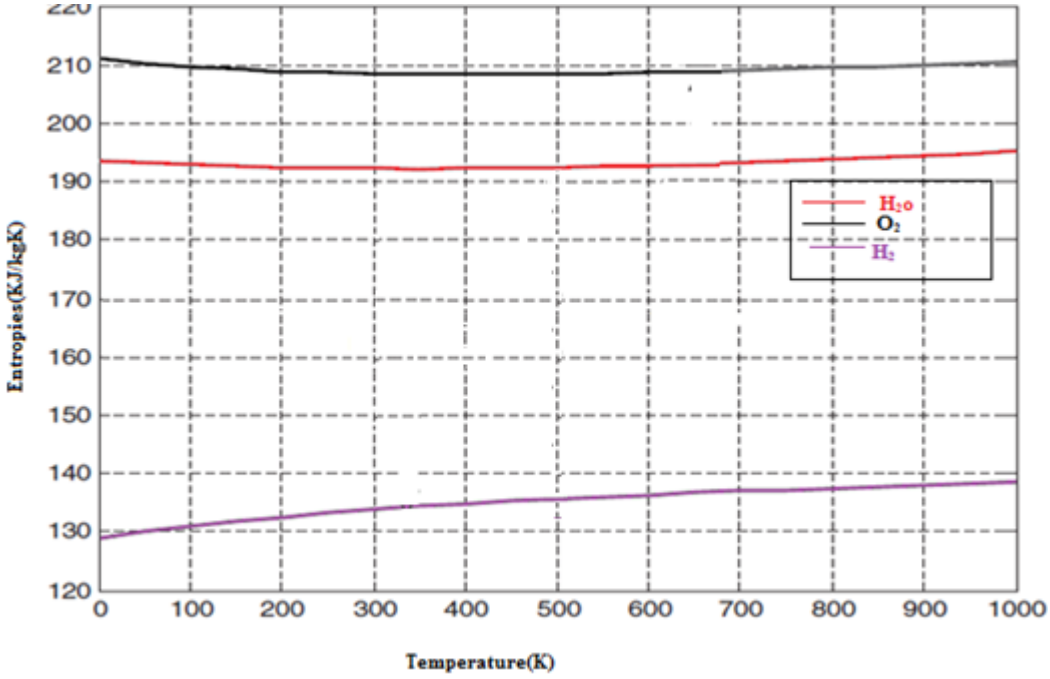

Graph 2.4 Entropy of H2,O2 and H2o versus temperature

Entropy of H_2, H_2o and O_2, in the above graph has obtained with the help of the parameter given in the table 2.1.

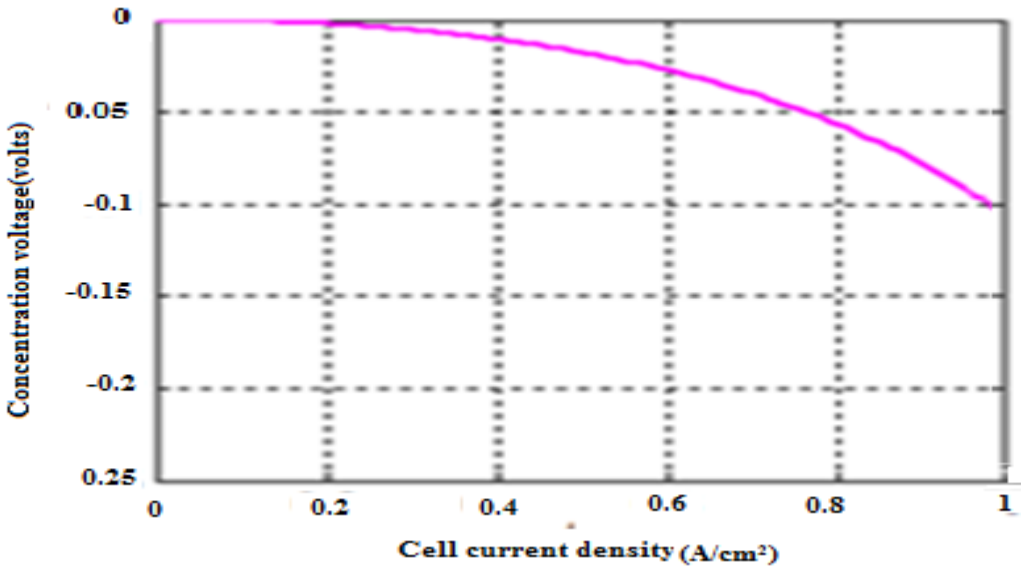

Graph 2.5 Concentration Loss versus cell current density

Concentration overvoltage of fuel cell in the above graph is decreasing with the increase in cell current density.

Summary:

Fuel cell is a renewable source of energy. Due to double charge layer effect, fuel cell can act like an ultra capacitor. There are different types of losses associated with fuel cell, which causes reduction in the cell voltage. In this chapter the modeling of different type of losses and thermodynamic potential has discussed. Dynamic model of fuel cell converted into the electric circuital model, consists of resistance (equivalent to losses), electrical capacitance and a voltage source (E_{Nernst}).

Chapter3

Buck and Boost Converter Circuit Topologies

Chapter 3

Buck and Boost Converter Circuit Topologies

3.1 Introduction

Buck and boost Converter used in **S**witched Mode Power Supply abbreviated as SMPS is nothing but a dc-to-dc switching converter for the conversion of unregulated dc input voltage to regulated dc output voltage. The switch employed in SMPS is turned 'ON' and 'OFF' (referred as switching) at a high frequency, with the help of an external switching circuit. During 'ON' state of the switch, the transistor acting as a switch will be in saturation mode with negligible voltage drop across the collector and emitter terminals of the switch, whereas in 'OFF' state the transistor acting as a switch will be in cut-off mode with negligible current through the collector and emitter terminals. Unlike in the voltage-regulating switch, a linear regulator circuit always remains in the active region, which results in low efficiency, only applicable to low power application. SMPS is well suited for high power applications.

3.2 Buck Converter working principle

The operation of the buck converter is very simple, with an inductor and two switches (a transistor and a diode) that control the inductor. Two switches come into action and alternate between connecting the inductor to voltage source to store energy in the inductor and discharging it into the connecting load. The inductor L and capacitor C in Fig.3.1 contributes into the filtering to avoid from the current, and voltage ripple respectively. Diode in the figure is a freewheeling diode, to ensure a continuous flow of the current into the circuit. The output voltage of the circuit can be controlled by the duty cycle D given by $D = \frac{t_{on}}{T}$. Output voltage v_o is always lower than input voltage v_i hence, we can also call this converter a "Buck Converter".

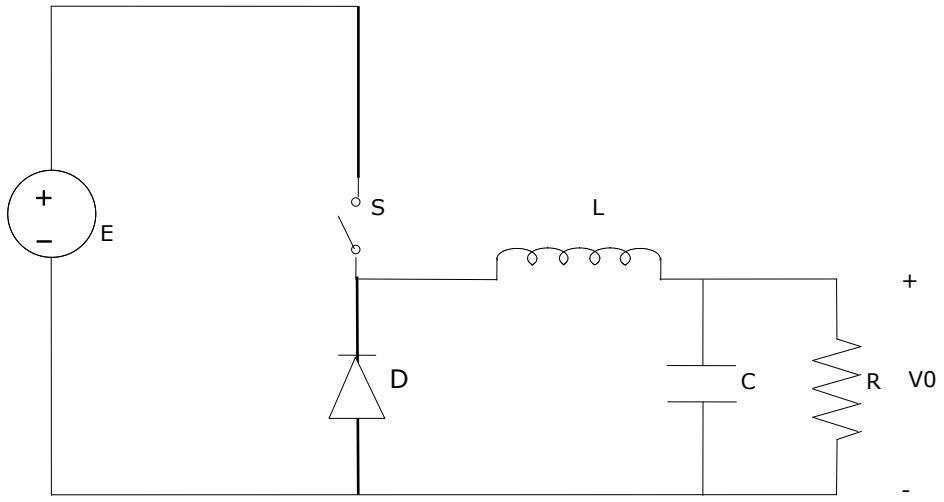

Fig.3.1 Schematic of Buck Converter

There are two basic modes in which Buck Converter operates:

(a) Continuous mode:

A buck converter operates in continuous mode if current through inductor never falls to zero, during the commutation cycle. Its operating principle is described by the Fig.3.2. When the switch shown above is closed, the voltage across the inductor is $v_l = v_i - v_o$. The current through inductor rises linearly. As the diode is reverse biased by the voltage source, no current flows through it.

When the switch is opened the diode D becomes forward biased.

Current i_L decreases.

The rate of change of current i_L can be calculated from:

$$v_L = L\frac{di_L}{dt} \tag{3.1}$$

Increase in current during on state can be calculated from [16]:

$$\Delta i_{L,on} = \int_0^{T_{on}} \frac{v_L}{L} dt = \frac{v_i - v_o}{L}.T_{on} \tag{3.2}$$

The decrease in inductor current is given by [16]:

$$\Delta i_{L,off} = \int_0^{T_{off}} \frac{v_L}{L} dt = \frac{-vo}{L}.T_{off} \tag{3.3}$$

The energy stored in each component at the end of commutation cycle T is the equal to that at the beginning of the cycle. That means current i_L will remain same at t=0 and t=T.

We can write the following equation with the help of above two equations as [16]:

$$\frac{v_i - v_o}{L} T_{on} = \frac{v_o}{L} T_{off} \tag{3.4}$$

$$(v_i - v_o).DT = v_o(1-D)T \tag{3.5}$$

Where; $D = \frac{T_{on}}{T}$ (3.6)

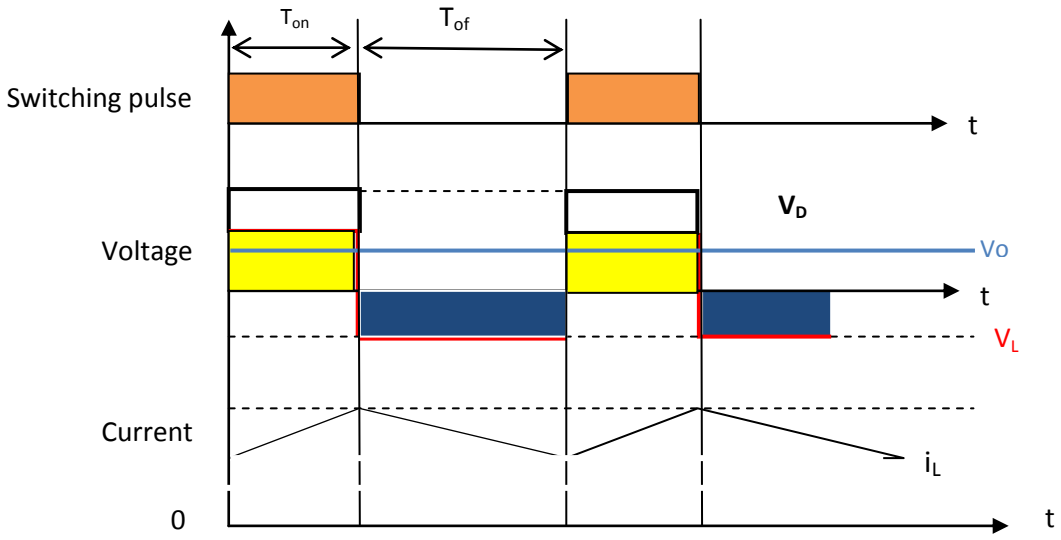

Fig.3.2 waveform of an ideal buck convert current and voltage in continuous mode

(b)Discontinuous mode:

Sometimes the energy required by the load is small enough to be transferred in a time lower than the commutation time. In this case the current through the inductor fall to zero before the commutation period (time period of the switch state).The various current and voltage component waveform is depicted in the Fig.3.3. In figure V_D is the voltage across the diode V_O is output voltage, V_L is the voltage across the inductor and i_L is the inductor current.

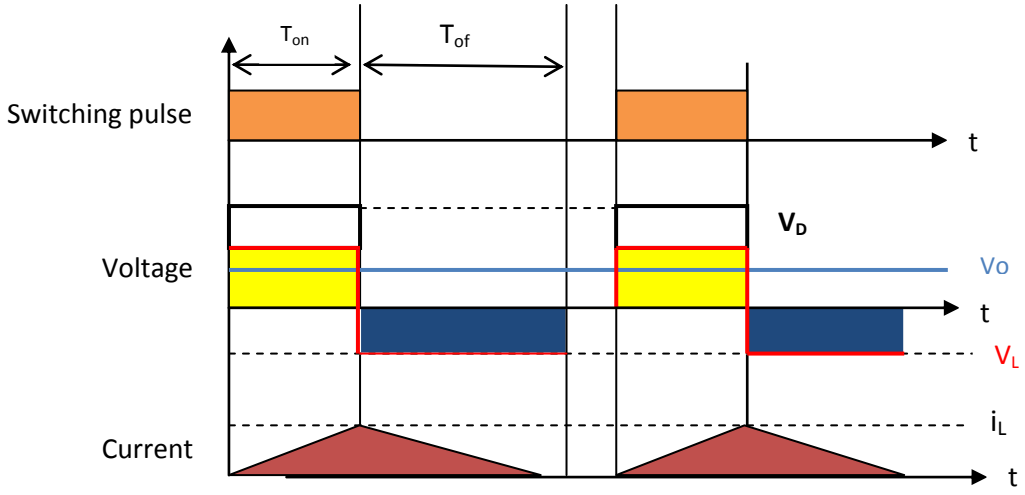

Fig.3.3 Voltage and current of an ideal buck converter operating in Discontinuous mode.

In this mode of operation inductor is completely discharged at the end of the commutation cycle.

$$(v_i - v_o).DT = v_o \delta T \tag{3.7}$$

So the value of $\delta = \frac{v_i - v_o}{v_o} D$ (3.8)

3.3 Boost Converter working principle:

A boost converter (in Fig.3.4) is a dc to dc voltage converter with an output dc voltage greater than input dc voltage. This is an SMPS containing at least two semiconductor switches (a diode which act as freewheeling diode two ensure a path of the current during the off state of other switch and a transistor connecting in series of the source voltage). Filters made of capacitor and inductor is used to reduce the ripple in voltage and current respectively, is used at the output stage of the converter.

Operating principle:

The basic operating principle of the converter consists of the two distinct states.

- In on state, switch is closed, resulting in an increase in the inductor current.
- In off state, switch is open, resulting in decrease in the inductor current.

There are two basic modes in which Boost Converter operates:

(a)Continuous mode:

As like the buck converter in continuous mode discussed above, in this mode of Boost converter, the current through the inductor (i_L) never falls to zero. Fig.3.5 shows a typical

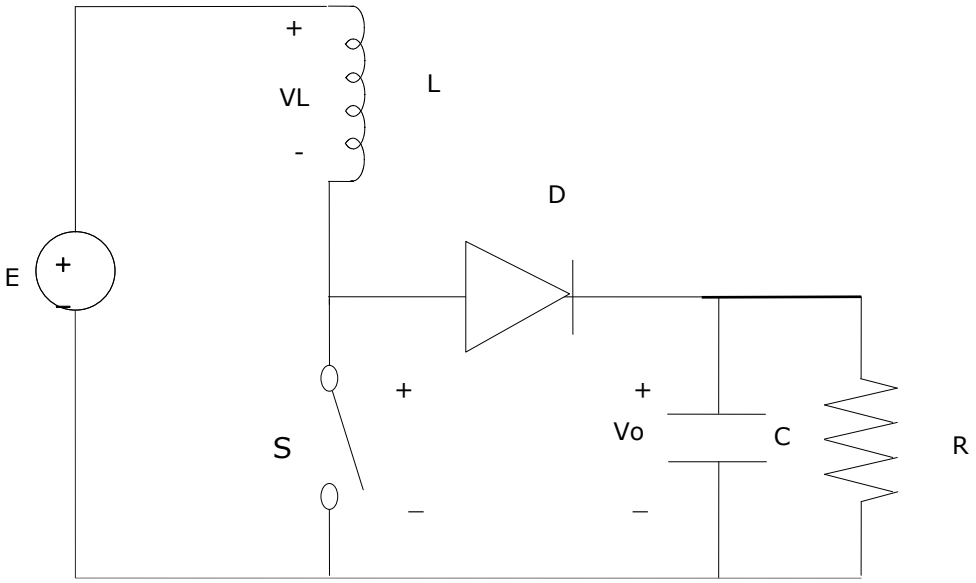

Fig.3.4 Boost Converter (step up chopper)

waveform of current and the voltages.

During the on state, switch S is closed, which makes the input voltage (v_i) appear across the inductor, which in turns results in change in inductor current (i_L) during a time interval Δt.Rate of change of current is given by [17]:

$$\frac{\Delta i_L}{\Delta t} = \frac{v_i}{L} \tag{3.9}$$

At the end of the on-state the increase in inductor current is given by [17] :

$$\Delta i_{L,on} = \frac{1}{L}\int_0^{DT} v_i \, dt = \frac{DT}{L} v_i \tag{3.10}$$

During the off-state, the switch s is open, so the inductor current flows through the load, the evolution of i_L, assuming voltage drop across diode is zero and a large capacitor is:

$$v_i - v_o = L\frac{di_L}{dt} \tag{3.11}$$

Variation of i_L during the Off-period is:

$$\Delta i_{L,off} = \int_{T}^{DT} \frac{(v_i - v_o)}{L} dt = \frac{v_i - v_o}{L}(1-D)T \tag{3.12}$$

The energy stored in each component at the end of commutation cycle T is the equal to that at the beginning of the cycle. That means overall change in current is zero [17]:

$$\Delta i_{Lon} + \Delta i_{Loff} = 0 \tag{3.13}$$

Substituting Δi_{Lon} and Δi_{Loff} by their expression in above equation we get [17]

$$\Delta i_{Lon} + \Delta i_{Loff} = \frac{vi}{L} DT + \frac{(vi - vo)}{L}(1-D)T = 0 \tag{3.14}$$

This can be written as [17]:

$$\frac{v_o}{v_i} = \frac{1}{1-D} \tag{3.15}$$

The above equation reveals that the output voltage will be always greater than input voltage.

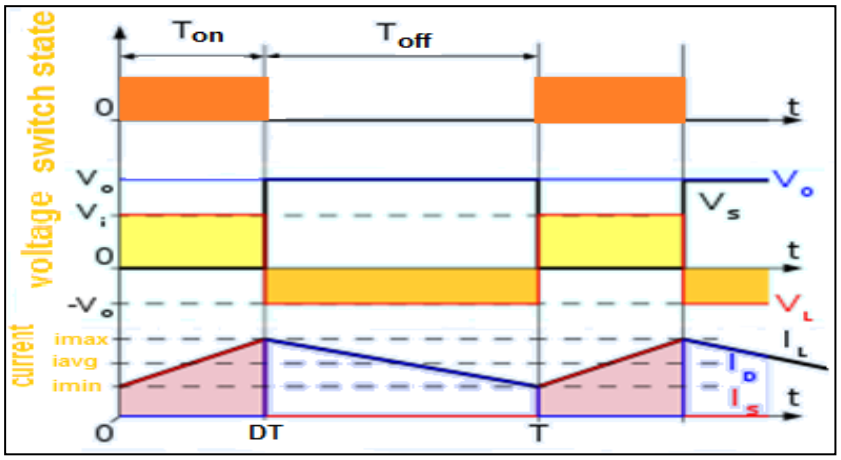

Fig.3.5 Voltage and Current of a Boost Converter operating in continuous mode.

(b)Discontinuous mode:

In this mode inductor current falls to zero during small part of the period. During the on-time, i_{Lmax} (at $t = DT$) is

$$i_{L\max} = \frac{v_i}{L} DT \tag{3.16}$$

During the Off-period, i_L falls to zero at δ T [17]

$$i_{L\max} + \frac{(vi - vo)\delta T}{L} = 0 \tag{3.17}$$

Using the two previous equations δ is:

$$\delta = \frac{v_i\ D}{vo - vi} \tag{3.18}$$

Load current is given by the average diode current [17]

$$i_{L\max} = \overline{i_D} = \frac{i_{L\max}\,\delta}{2} \tag{3.19}$$

Replacing i_{Lmax} and δ by their respective expressions the following relation yields [17]:

$$i_o = \frac{v_i DT}{2L} \cdot \frac{v_i D}{vo - vi} = \frac{v_i^2 D^2 T}{2L(v_o - v_i)} \tag{3.20}$$

Output and input voltage ratio can be expressed as [17]:

$$\frac{v_o}{v_i} = 1 + \frac{v_i D^2 T}{2L i_o} \tag{3.21}$$

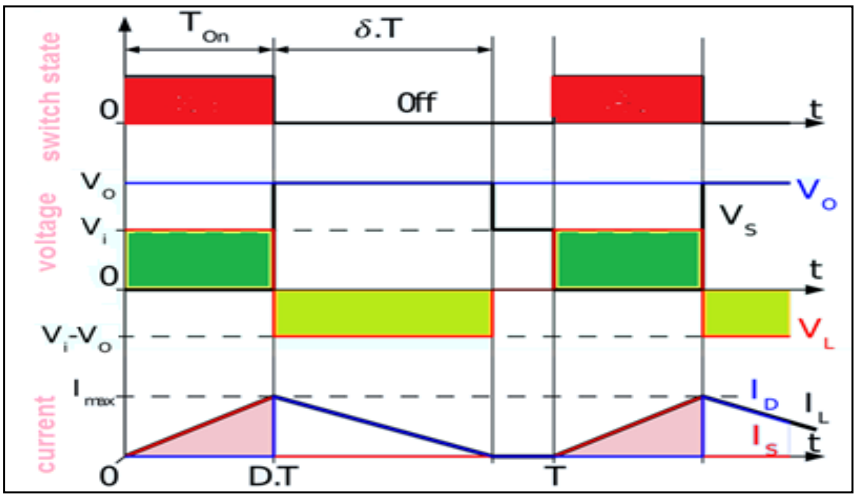

Fig.3.6 Voltage and current of a Boost Converter operating in discontinuous mode.

3.4Simulink model of Buck Converter:

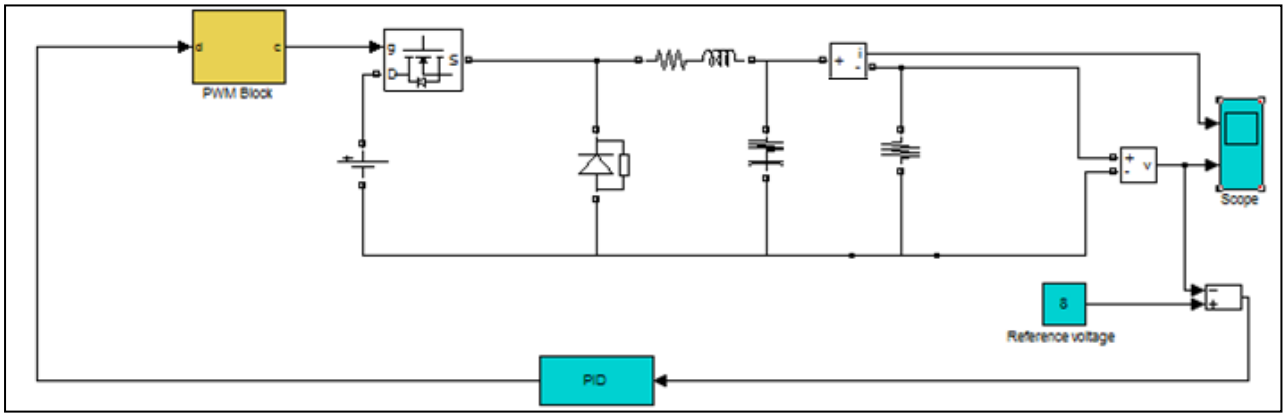

Fig.3.7 Simulink model of Buck converter

Above Simulink model has simulated with the converter parameter value given in table 3.1. Voltage and current of the above Simulink model of buck converter is shown in Fig.3.8

Table 3.1

Converter parameter	Value
Source voltage	12 (v)
Reference voltage	8 (v)
L	4.1 µH
RL	3e-4 Ω
C	300 µF
RC	5e-3 Ω
f_s	100 kHz
Load resistance	1 Ω

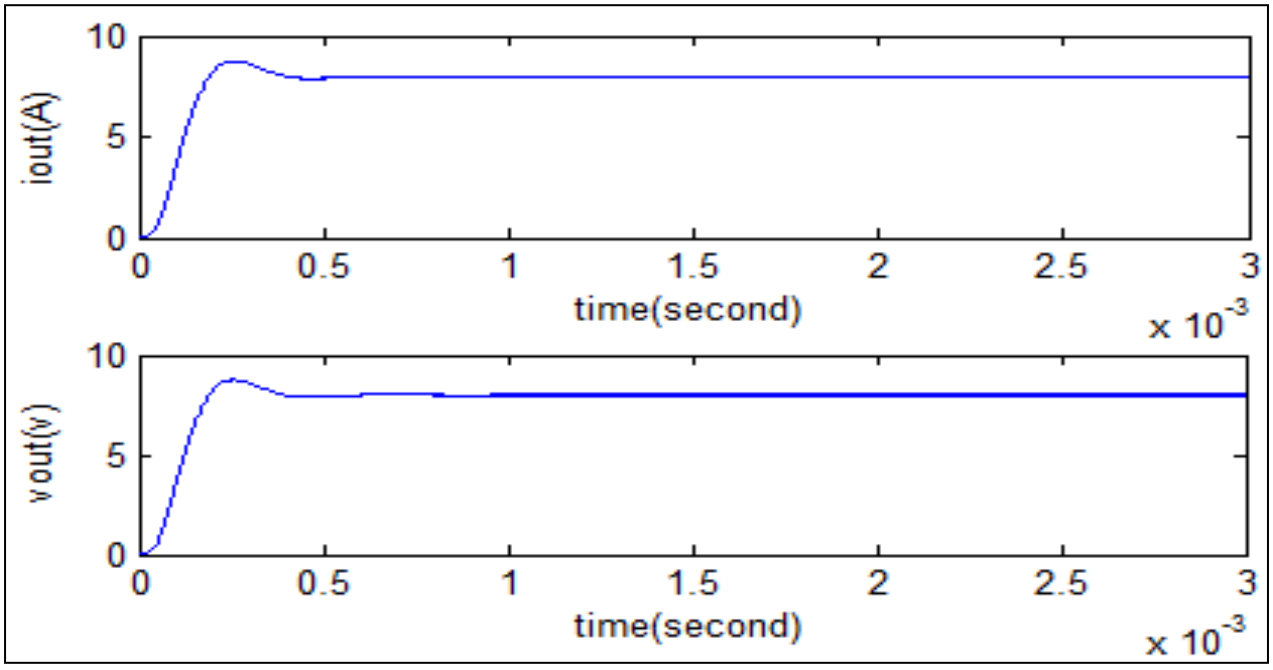

Fig.3.8 Voltage and current of the buck converter (shown in fig.3.7)

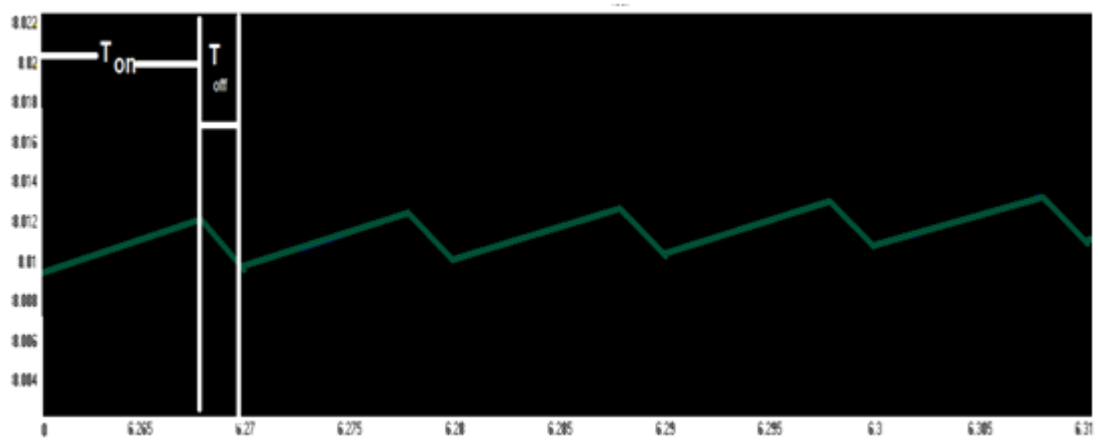

Fig.3.9 Buck converter voltage at steady state

Result description:

Output voltage = 8.0015 v.

At $t = 7.5X10^{-4}$ s voltage reached at its steady state.

At steady state condition (shown in Fig.3.14):

Output current ripple = 8.0017 (A)-7.9967 (A) = 0.0050 (A)

Voltage ripple = 8.0012 (v)-7.999 (v) =0.0022 (v)

T_{on} = .00000066 s

T_{off} =.00000034 s

T = 10^{-5} s.

Duty cycle $D = \frac{T_{on}}{T} = \frac{66X10^{-7}}{10^{-5}} = .66$

Output voltage of Buck Converter is given by the relation:

$v_{output} = D.v_{input}$

$= .66X12\,(v) = 0.792\ (v).$

This is approximately equal to our reference voltage (8 v).

3.5 Simulink model of Boost Converter:

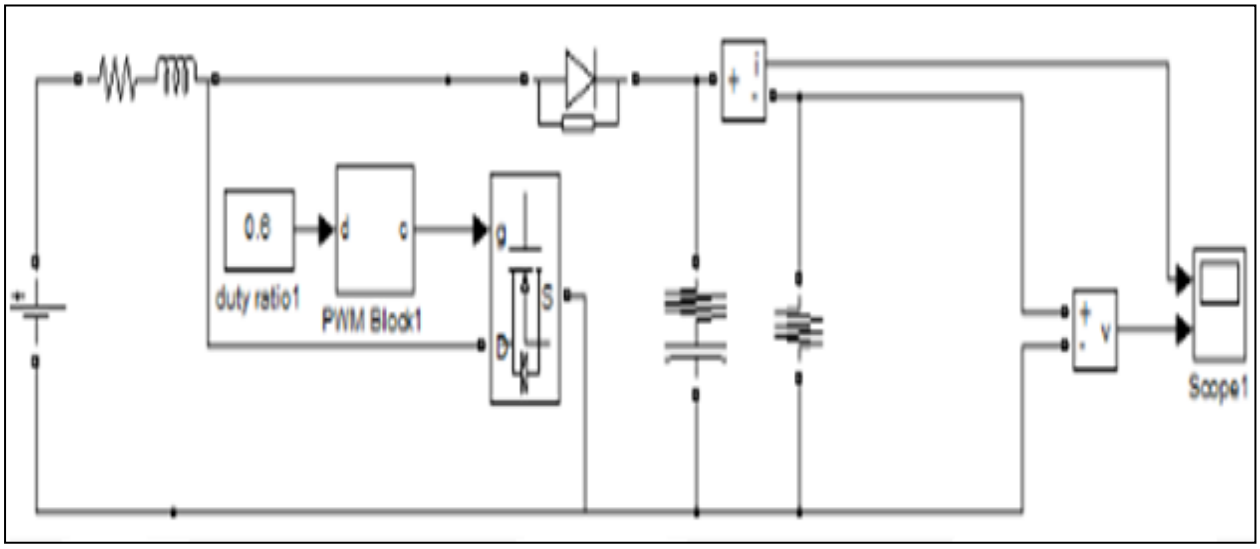

Fig.3.10 Open loop Boost Converter

Value of converter parameters, which we have taken in order to simulate the Simulink model shown in Fig.3.10 is given in table 3.2.

Table 3.2

Converter parameter	Value
L	75 µH
R_L	80 mΩ
RC	5 mΩ
C	1.68 µF
Fs	100 kHz
Vs	5 v
Load resistance	120 Ω
Reference voltage	12 v
Duty cycle	0.6

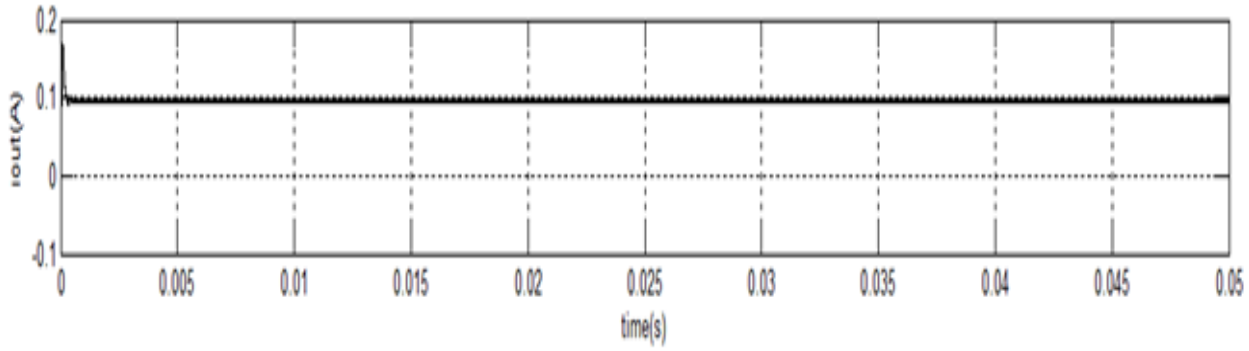

Fig.3.11 Output current of the Boost converter(shown in Fig.3.10)

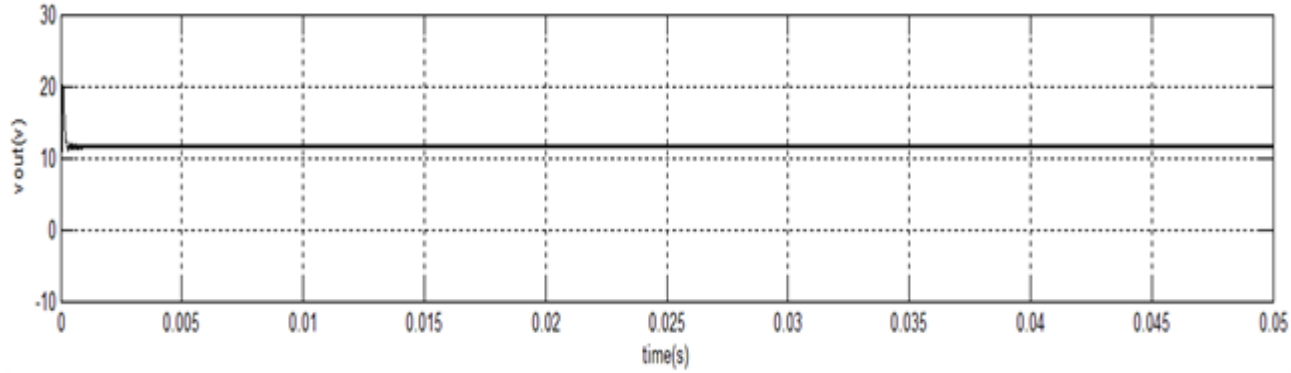

Fig.3.12 Output voltage of the Boost converter(shown in Fig.3.10)

Result Demonstration of Boost converter shown in Fig.3.10:

D =.61

Voltage to be regulated = 5 v

Reference voltage = 12 v

$$v_{out} = \frac{v_{in}}{1-D} = \frac{5}{1-.61} \approx 12v$$

=>Reference voltage $\approx$ output voltage.

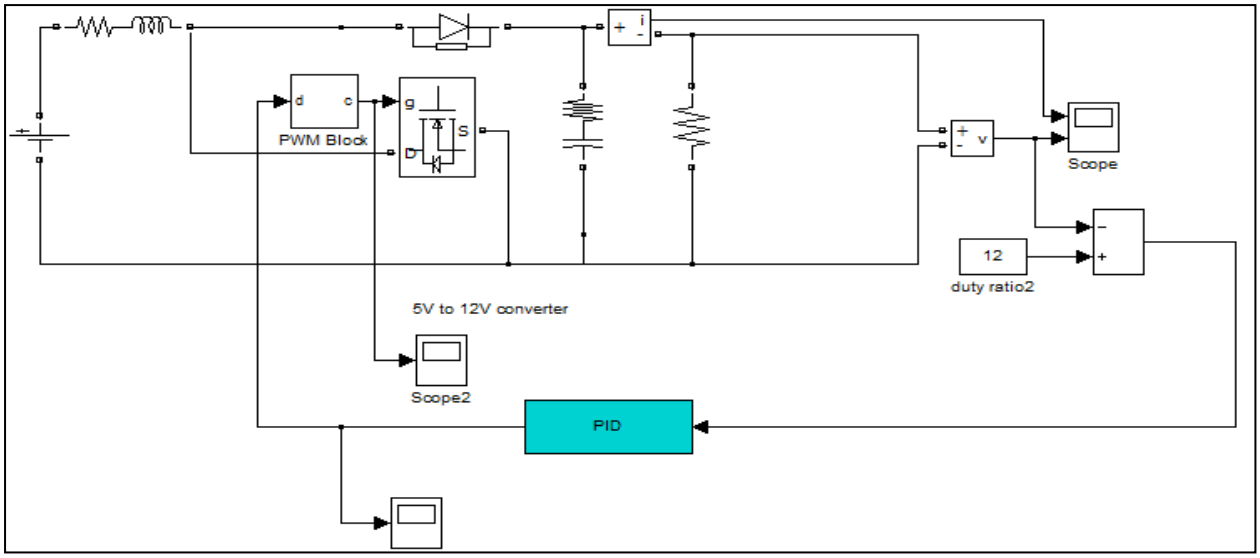

Fig.3.13 Simulink model of Closed Loop Boost Converter

Value of parameters that we have taken in order to simulate the Simulink model shown in Fig.3.13 is given in table 3.3.

Table 3.3

Parameter Name	**Value**
Source voltage	**5 (v)**
Reference voltage	**12 (v)**
f_s (PWM frequency)	**100 kHz**
Proportional constant of PI controller	**0.1**
Integral constant of PI controller	**0.34**
Inductance(L)	**159.8 µH**
Capacitance(c)	**225 µF**
RL(resistance in RL branch)	**80e-3 Ω**
RC(resistance in RC branch)	**5e-3 Ω**
Load Resistance	**10 Ω**

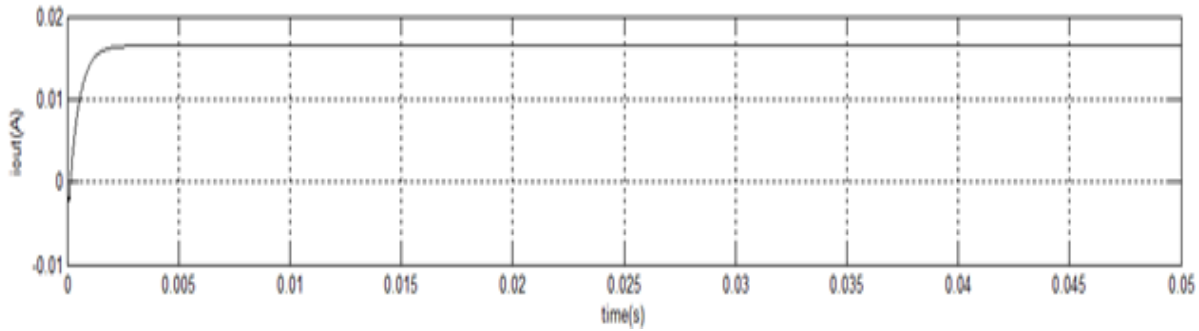

Fig.3.14 Output current of closed loop Boost Converter (in Fig.3.13)

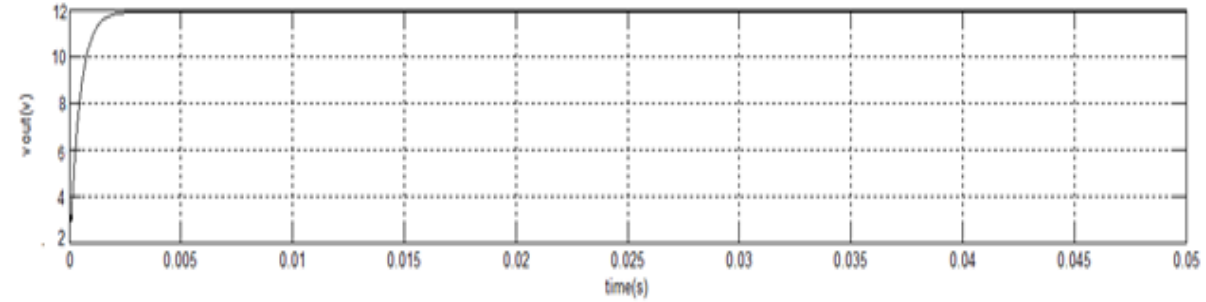

Fig.3.15 Output current of the closed loop Boost Converter (in Fig.3.13)

In close loop converter a PID controller is introduced to set the duty-cycle value, so that output voltage immediately follows the reference voltage.

Closed loop converter including PID controller is a better solution for a system, where input voltage is changing with any parameter. This controller adjusts the duty cycle of PWM by scaling the error signal by some factor, depending upon previous error.

Summary:

Different types of switching mode power supply have studied in this chapter. These converters are like dc equivalent of AC transformer, with an objective, to convert the input dc source from one level to another level efficiently. Closed loop converter, with a PID controller is well suited for the application where input voltage is varying with some of the source parameter and another converter parameter.

Chapter 4

Fuel Cell System

Chapter 4

Fuel Cell System

4.1 Introduction

A fuel cell power system (Fig.4.2**)** is a closed loop system, consisting of fuel cell stack, a PI+PWM controller and a converter, because the direct current (dc) output of a fuel cell stack will rarely be suitable for direct connection to an electrical load, so some kind of power conditioning is always required. This may be as simple as a voltage regulator, or a dc-dc converter. This thesis deals with a boost type power conditioner, which is discussed in chapter three. The switching of the boost converter is done through a PI+PWM controller. In this thesis we have simulated two models of fuel cell. In first model we have taken a time varying flow rate, and in second model we have taken switched load to simulate the behavior of fuel cell under time varying load.

4.2 Modeling of Fuel Cell System Using Matlab/Simulink

Fuel cell block in Fig.4.1 is modelled using the holistic modeling described in the chapter second.

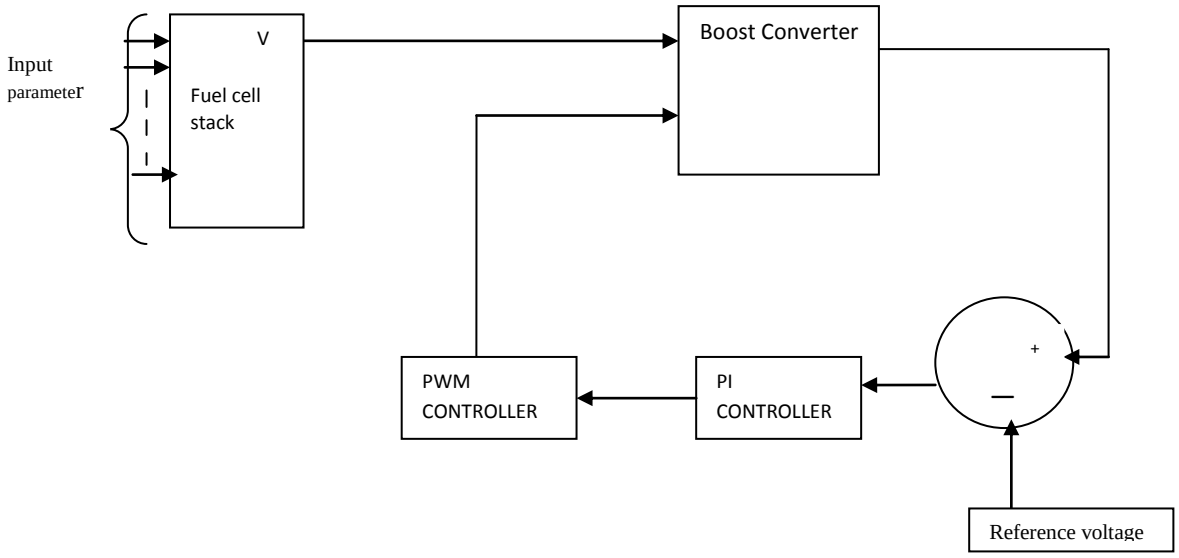

Fig.4.1 Block Diagram of closed loop fuel cell system

The whole model of fuel cell stack consists of two parts, as described in chapter 2 in section 2.3. Dynamic model of one fuel cell based on the electrochemical model of fuel cell is [1]:

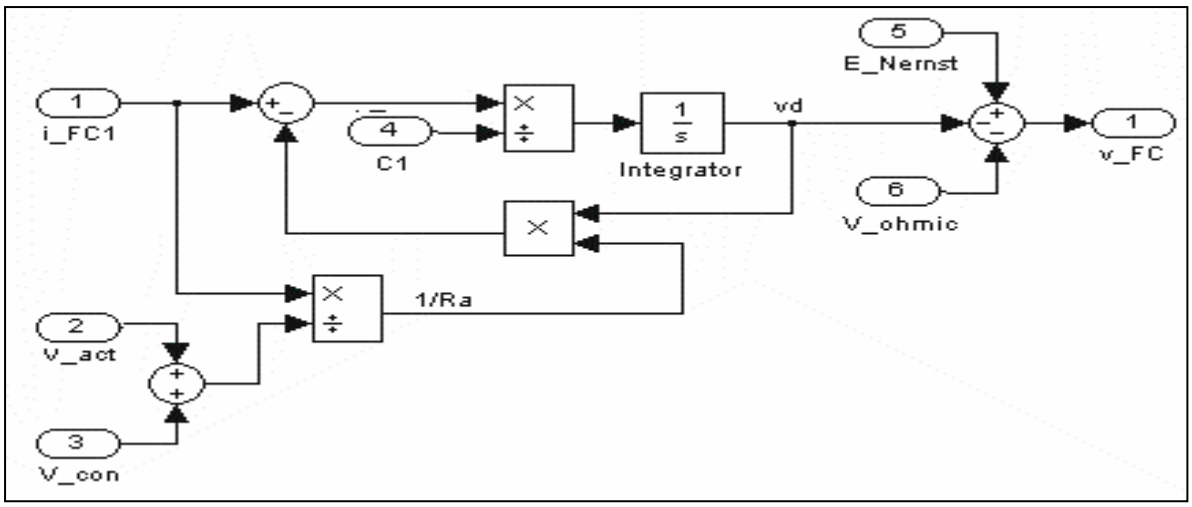

Fig.4.2 Dynamic model of fuel cell

4.3 Simulation of fuel cell model under time varying load

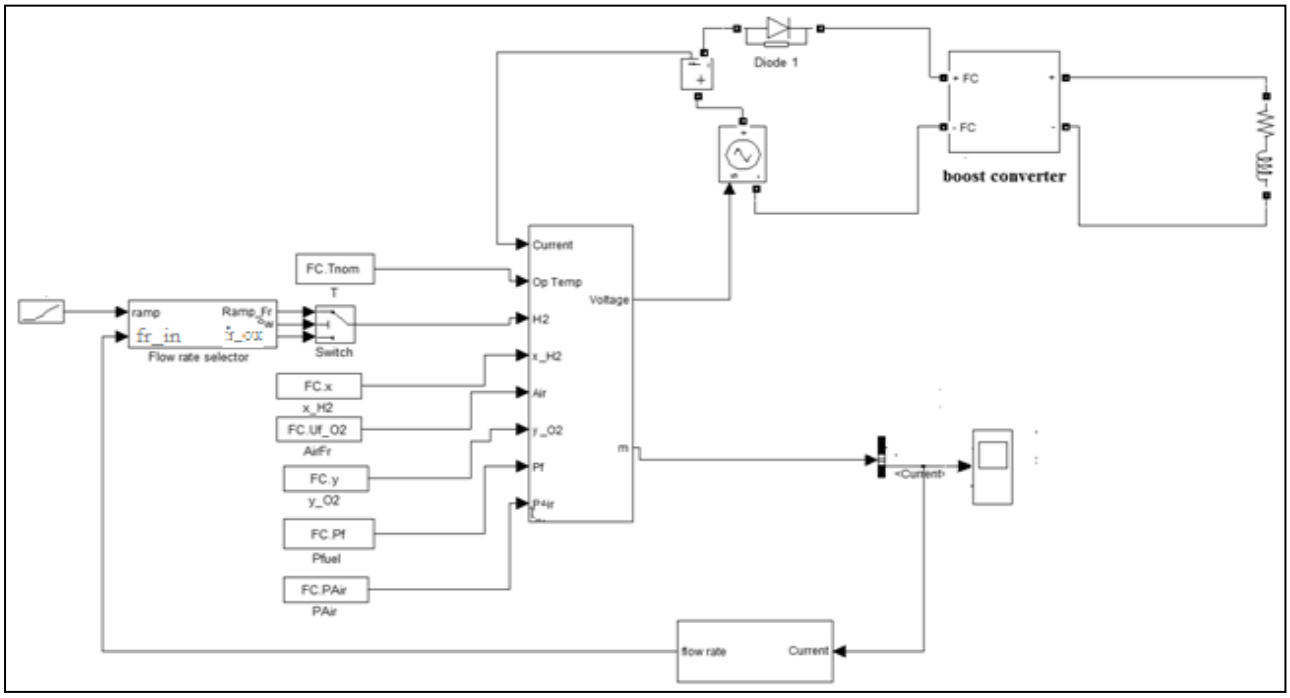

Fig.4.3 Simulink model of fuel cell system with varying flow rate

Whole fuel cell system model is shown in Fig.4.3, consists of a stack of 68 fuel cell, a 48 v to 96 v boost converter, flow rate regulator and selector, a controller consists of PI+PWM to control the switching action of boost converter.

We used Simulink model shown in Fig.4.3 to examine the effect of flow rate variation. In this model we have taken a flow rate regulator, and a flow rate selector. Model of flow rate selector is shown in Fig. 4.4.

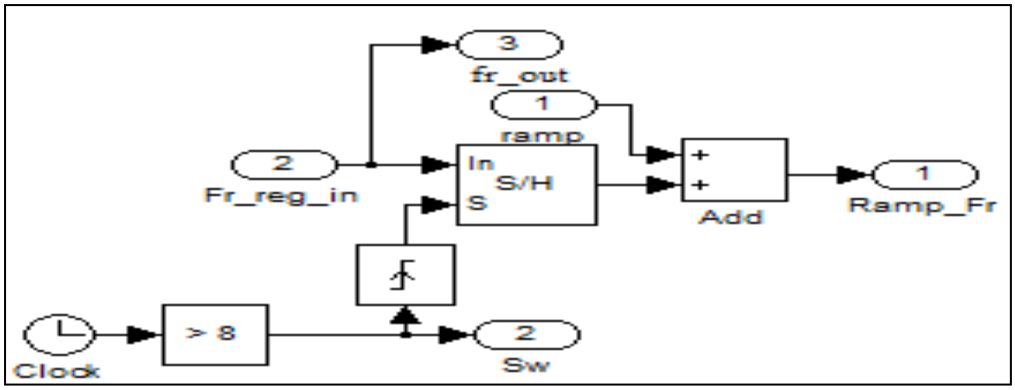

Fig.4.4 Model of flow rate selector

- **Relation of flow rate with current is given by the relation:**

Flow rate (lpm) =60000.R.T.Nc.i_fc/ (2F. (Pf.101325).Uf_H2/100.x/100) (4.1)

Where: R = Gas constant,

T = temperature in (k)

F = Faraday's constant

Pf = fuel pressure (bar)

Uf_H2 = fuel (H_2) utilization factor

Nc = Number of fuel cell in stack

i_{fc} = Fuel cell current (A).

The closed loop boost converter (Fig. 4.5) consists of an inductor of 500 µH, a resistance of 2 Ω and capacitance of 8000 µF, a low pass filter, which has a transfer function $\frac{1}{0.001S+1}$, a PI controller, discrete PWM generator and a switch (transistor).

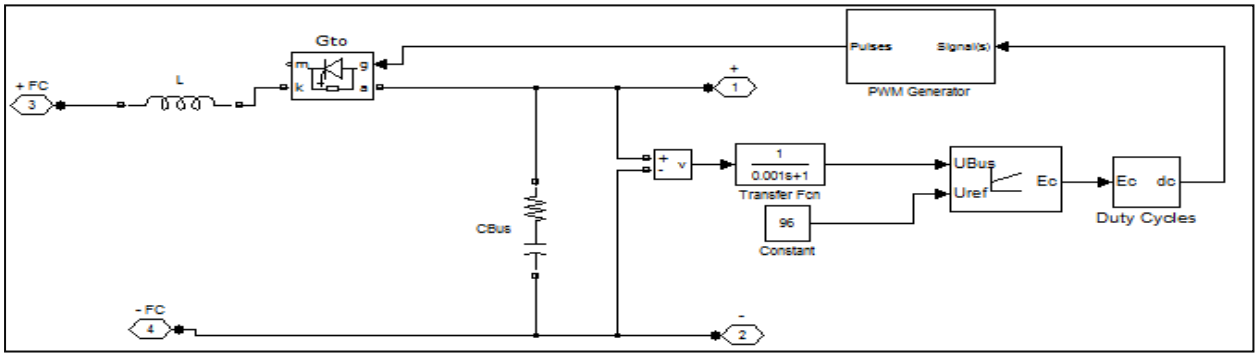

Fig.4.5 Model of boost Converter

PI controller is used to control the duty cycle by scaling the error voltage, finally the output stage of the converter is loaded by RL element of 2.4 kW and a time constant of 1 sec (R=L=v_{boost}^2/power =$(96)^2$/2400).Transfer function of PI controller is given by:

$$G_{PI} = K_P\left(\frac{1}{1+K_I s}\right) \quad (4.2)$$

Where K_P is proportional gain, which we have taken 0.005 and K_I is integral gain, that we have taken 0.15.

Fuel cell parameters that we have taken for simulation

Table 4.1

PEM fuel cell parameter	**Value**
Operating Temperature (Op_temp)	338 K
Fuel flow rate	Maximum 85 lpm (litre per minute)
Composition of fuel	99.95%
Air flow rate	372 lpm (litre per minute)
Composition of air	21%
pressure of air	6 bar
pressure of fuel	1 bar
Limiting current	0.00578 A
Area of fuel cell stack	50.6 cm^2
ψ	14
ξ_1	-0.9477
ξ_2	0.0033
ξ_3	$7.5X10^{-5}$
ξ_4	$-1.915\ X10^{-4}$
Equivalent capacitance	3F
Thickness of membrane	0.0178 Cm
R_{pr}	0.0003 Ω
B	0.016 (v)
Number of fuel cell in stack	68

The parameter, ψ can have a value as high as 14 under ideal, 100% relative humidity conditions [5].

4.3.1 Simulation Results of the fuel cell system model with varying flow rate :

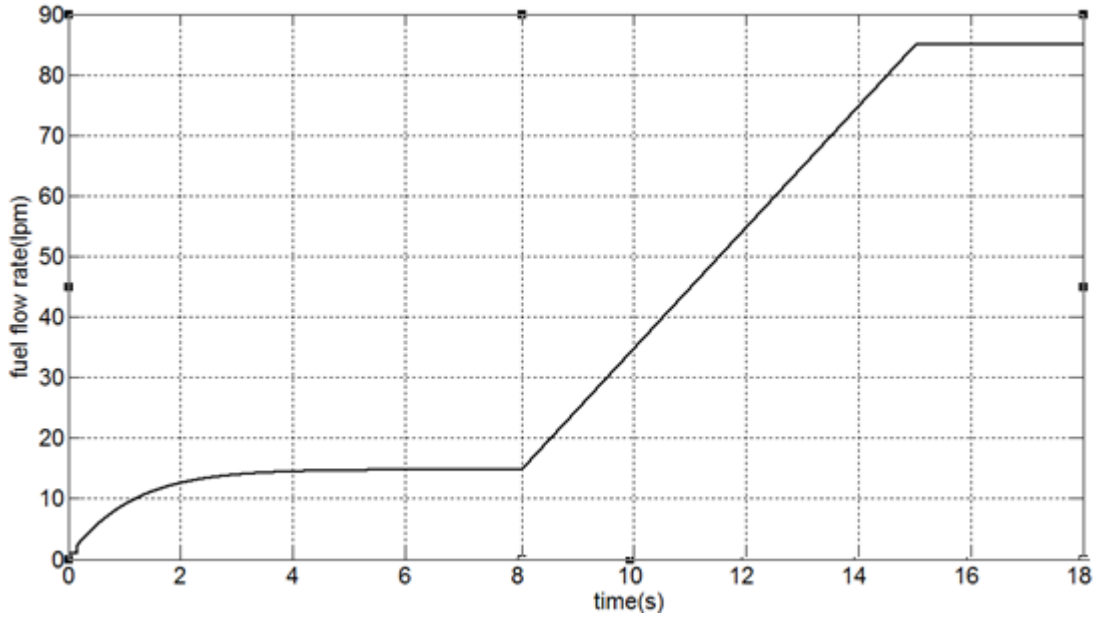

Graph 4.1 Flow rate versus time

In the above graph flow rate has changed at 8 s, from 16 lpm to 85 lpm, during the time interval 3.5 s.

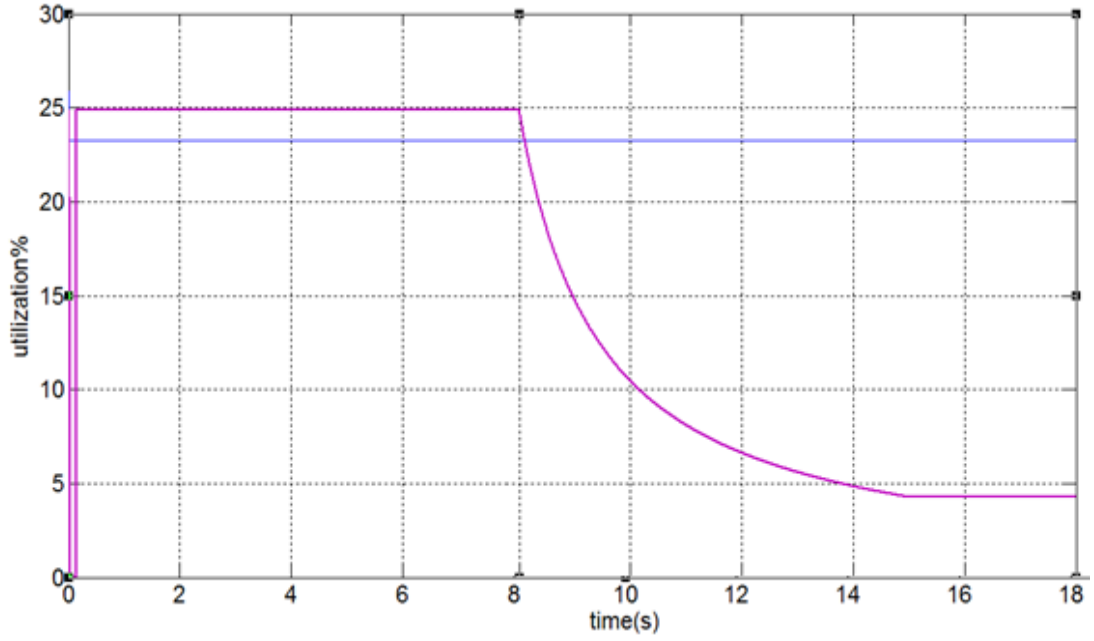

Graph 4.2 Utilization of fuel and oxidant (air)

Cell utilization is defined as $u = \frac{N_{H2}^{in} - N_{H2}^{0}}{N_{H2}^{in}}$

We observed in Graph4.2, as the fuel flow rate has increased utilization of fuel has decreased.

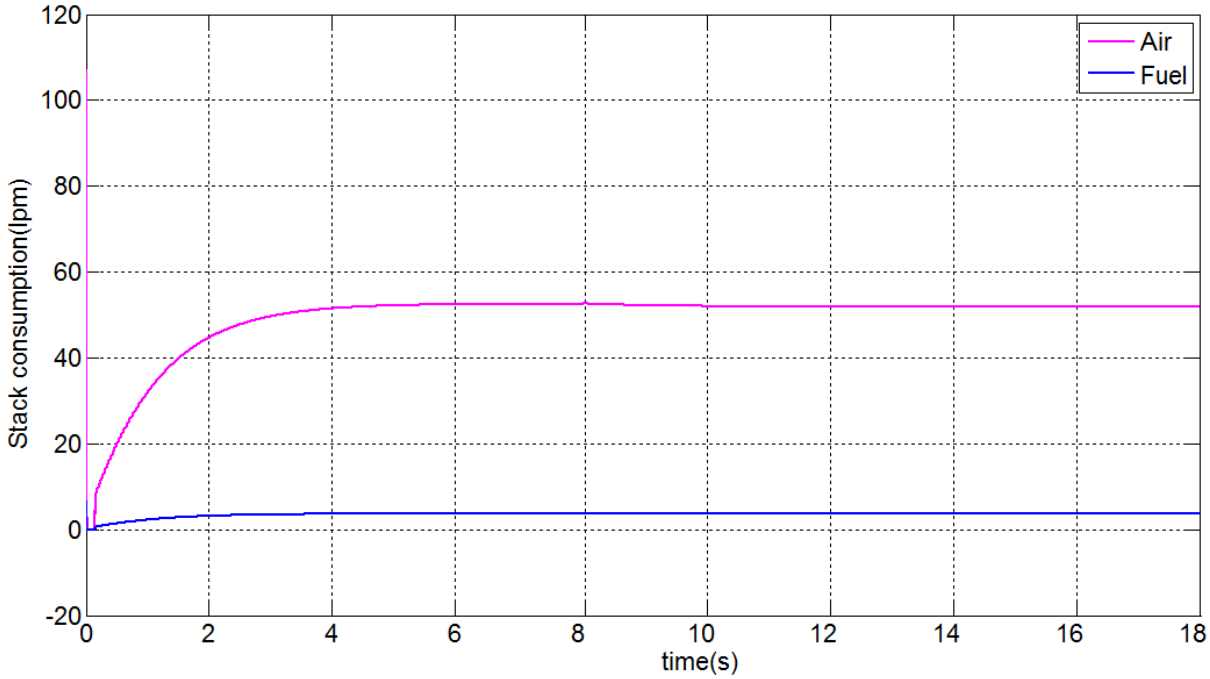

Graph 4.3 Consumption of fuel and oxidant(air) versus time

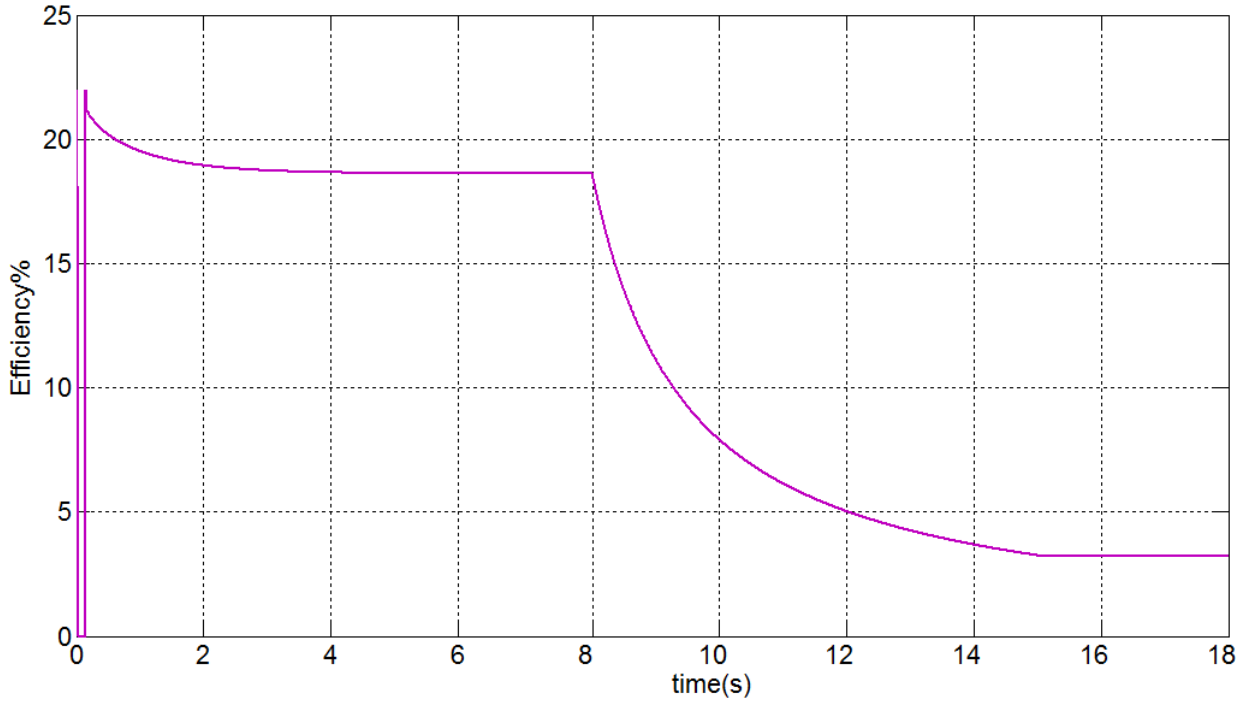

Graph 4.4 Stack efficiency versus time

Stack efficiency of the fuel cell system is defined as the ratio of maximum rated power to the power taken at the load. It has (shown in Graph 4.4) decreased with increase in flow rate of fuel.

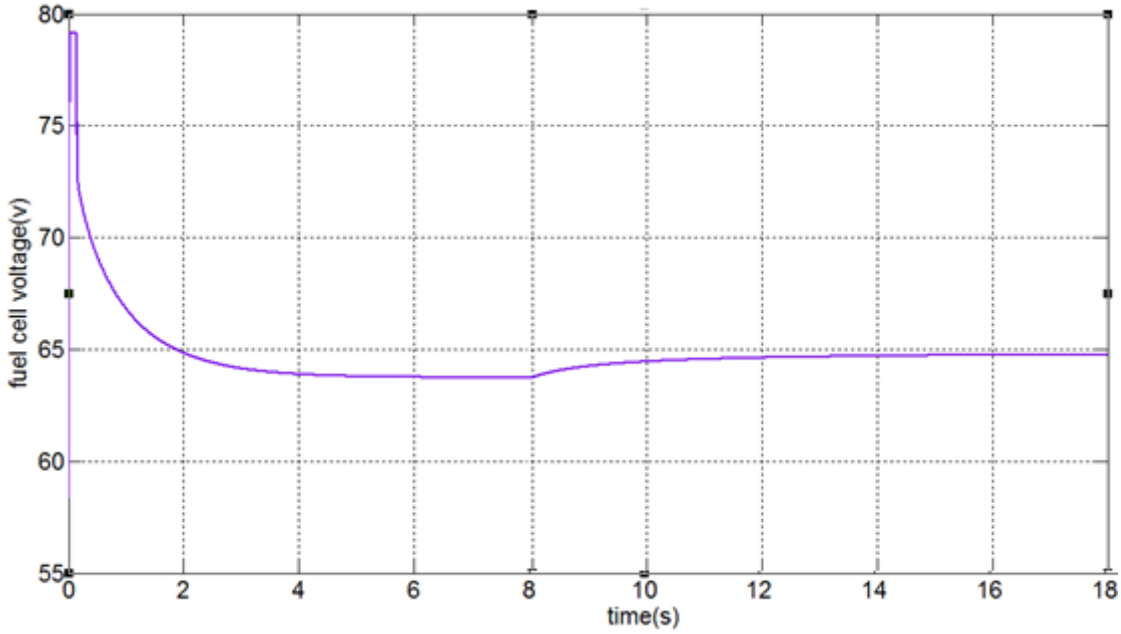

Graph 4.5 Fuel cell voltage versus time

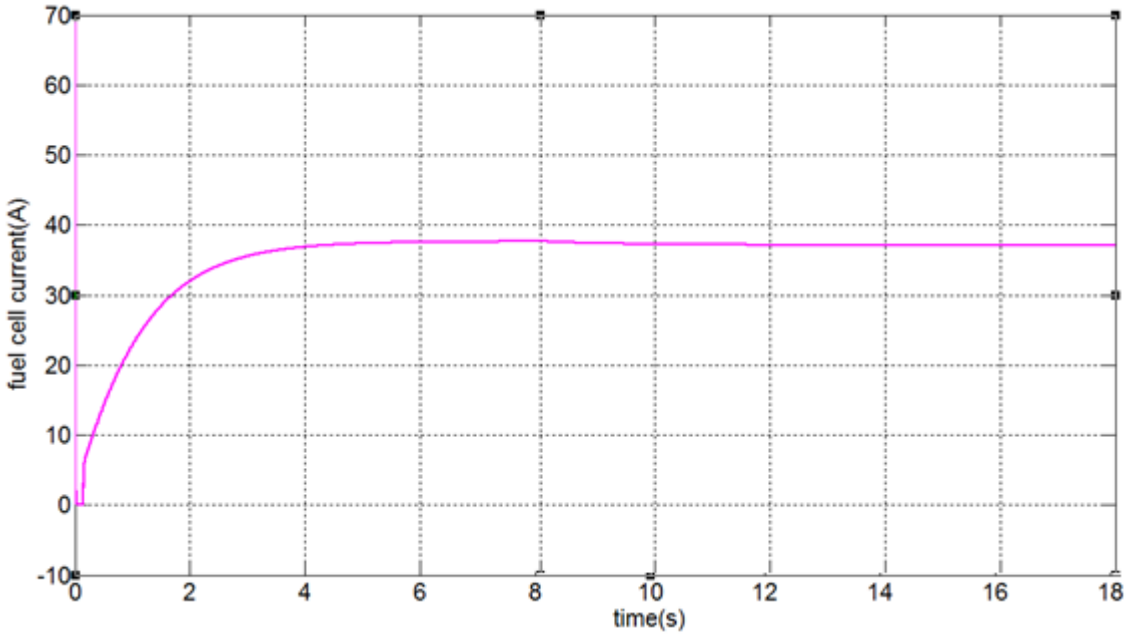

Graph 4.6 Fuel cell current versus time

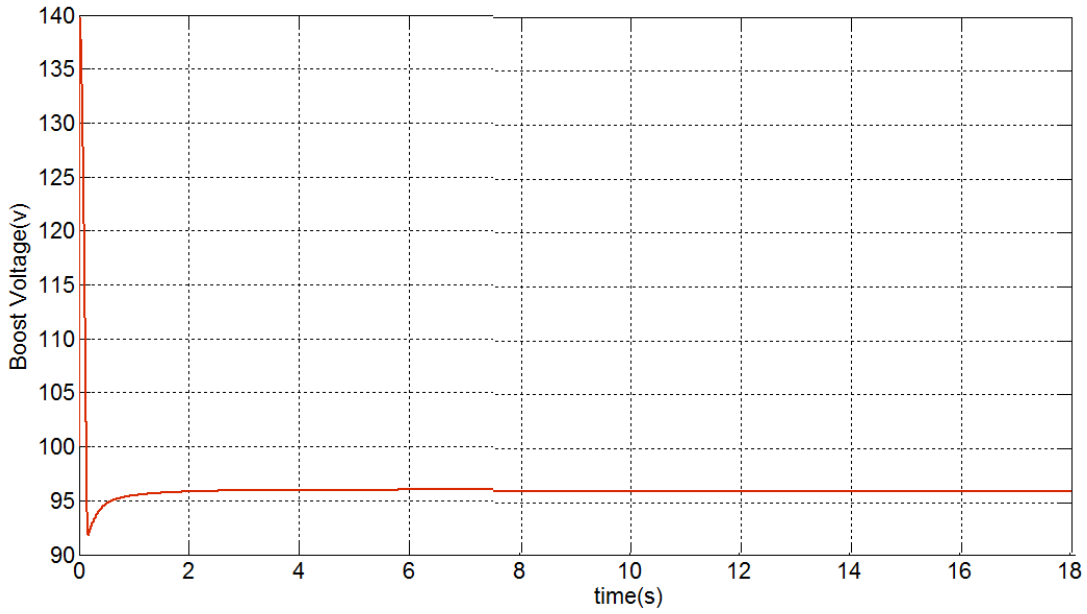

Graph 4.7 Boost output voltage versus time

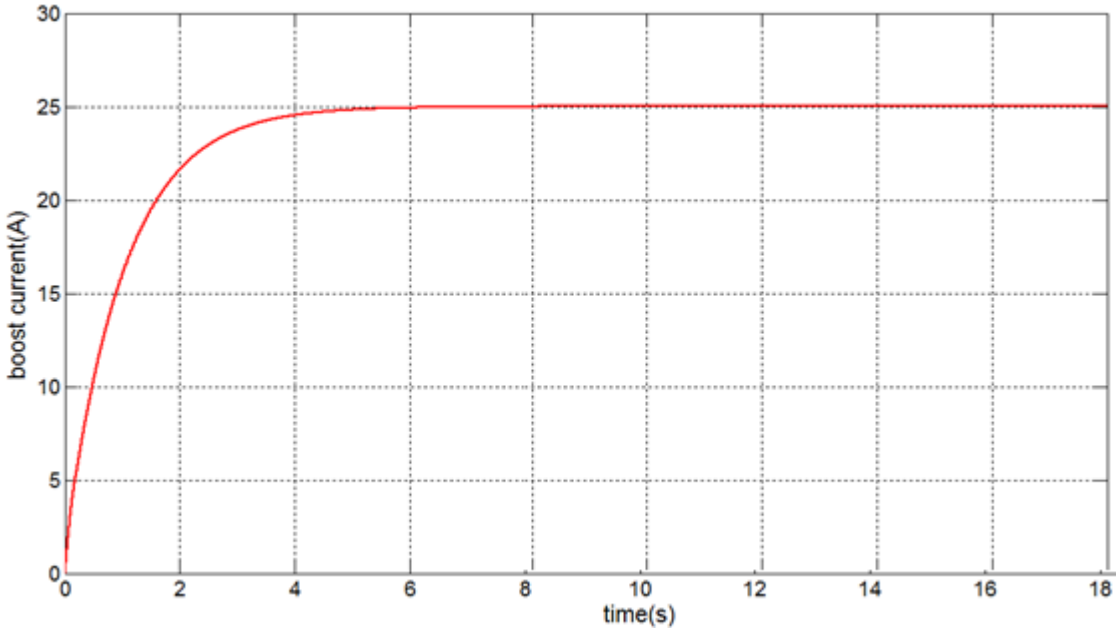

Graph 4.8 Boost output current versus time

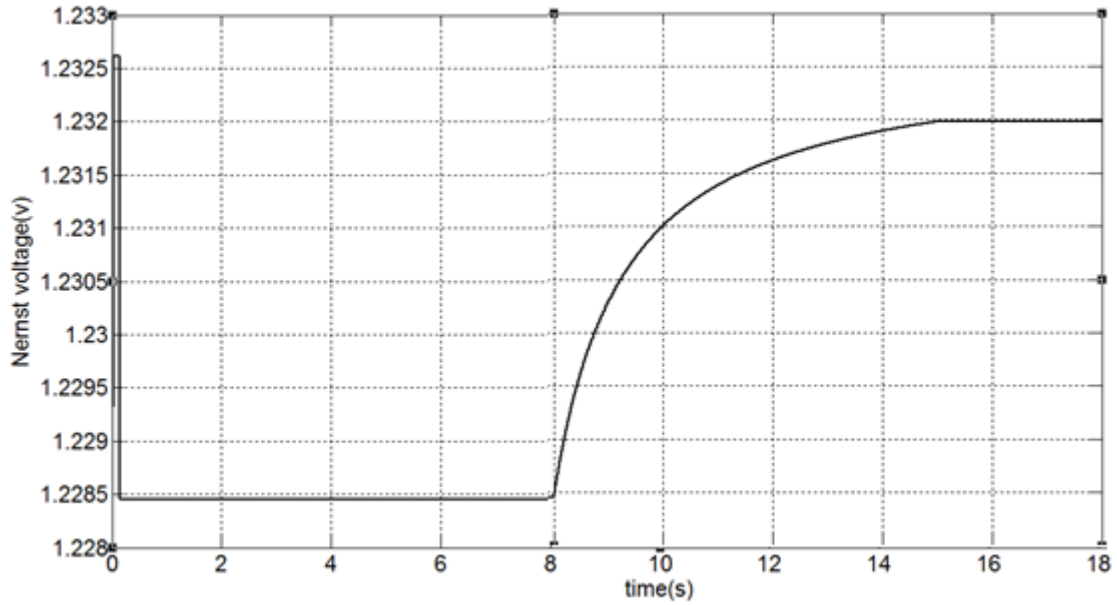

Graph 4.9 Nernst voltage versus time

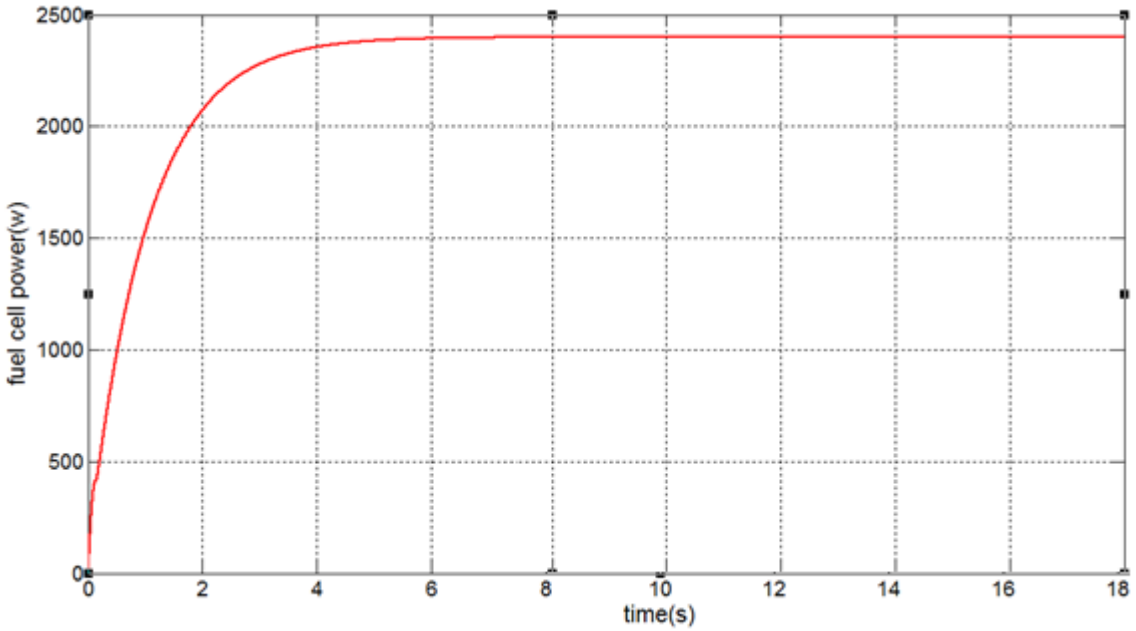

Graph 4.10 Output power versus time

4.3.2 Result Demonstration

At t = 0 s, the dc-dc converter applies 96 v dc to the RL load (the initial current of the load is 0A). The current (Graph 4.6) increases until the value of 35 A. The flow rate is automatically set in order to maintain the nominal fuel utilization. The dc bus voltage is very well regulated by the converter (Graph 4.7). The peak voltage of 132 v dc (Graph 4.7) at the beginning of the simulation is caused by the transient state of the voltage regulator.

At t = 8 s, the fuel flow rate is increased from 18 litres per minute (lpm) to 85 lpm during 3.5 s (Graph4.1), reducing by doing so the hydrogen utilization (Graph 4.2). This causes an increasing of the Nernst voltage (thermodynamic potential) (Graph 4.9), so the fuel cell current will decrease (Graph 4.6). Therefore the stack consumption (Graph 4.3) and the efficiency (Graph4.4) will decrease.

4.4 Simulation of fuel cell system model under time varying load

In order to simulate the fuel cell system under the variation of load, we have taken another Simulink model (Fig. 4.6) to examine the regulation of the output voltage with the variation of the load with time.

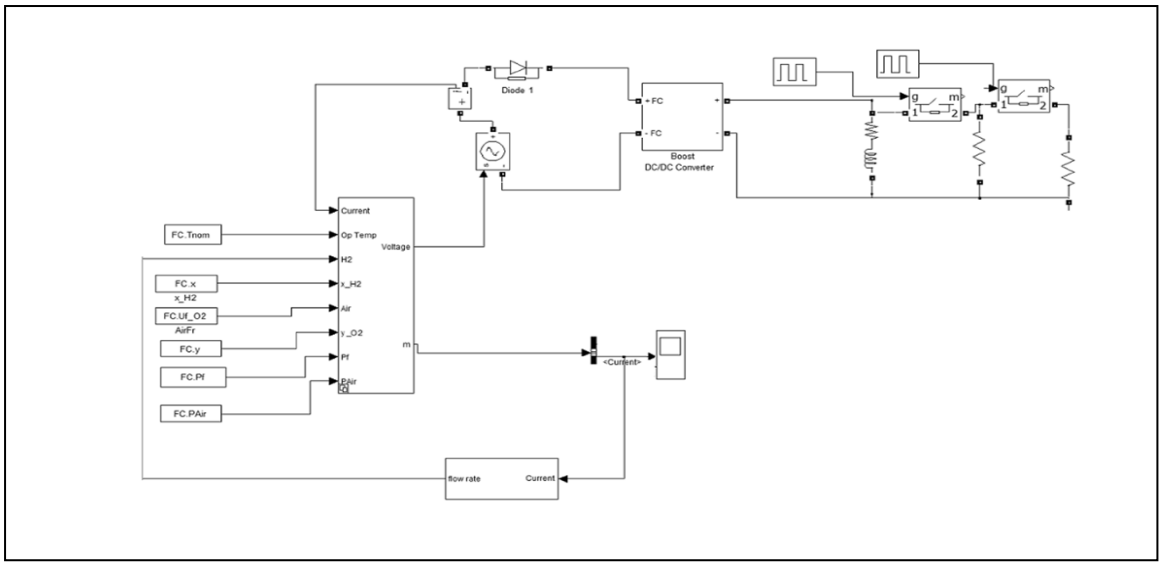

Fig.4.6 Simulink model of fuel cell system under switched load

In this Simulink model we have used the entire component same as first Simulink model, except for the time varying load. The variation of the load is done through two parallel load connecting at the terminal of the RL load, whose connectivity is changed at a regular interval of 5 s with the help of a switch, to see the changes in the output voltage, current and the rated power.

4.4.1 Simulation Results

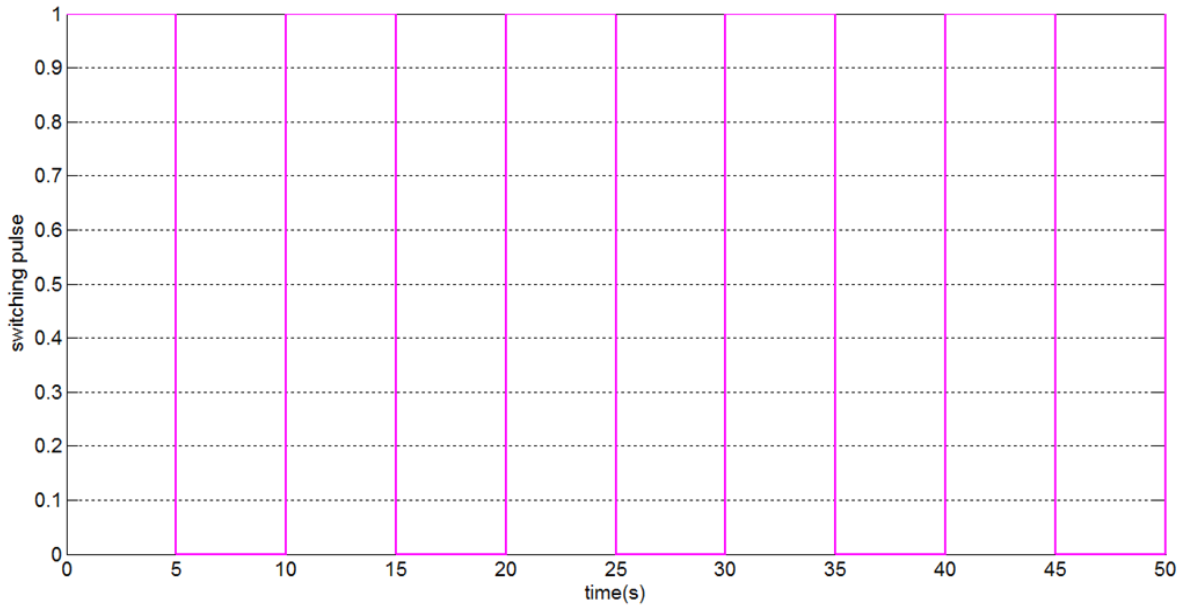

Graph 4.11 Load switching pulse

Switching of the load of fuel cell system has done through the switching pulse, shown in the Graph 4.11.

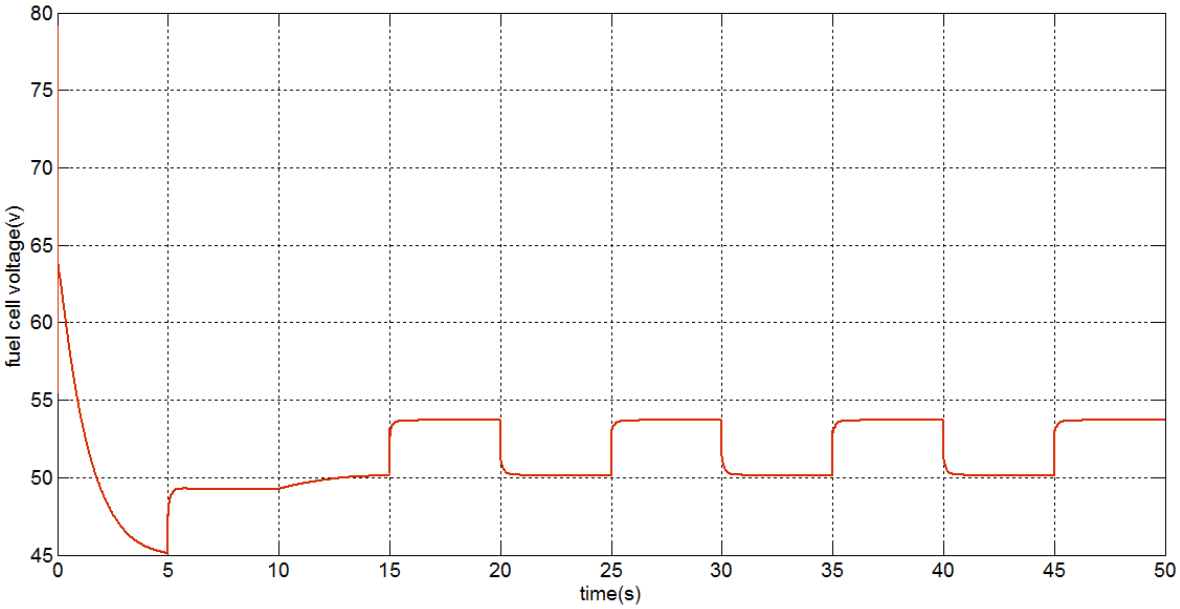

Graph 4.12 Fuel cell voltage versus time

With the change of load, fuel cell voltage has changed (shown in Graph 4.12)

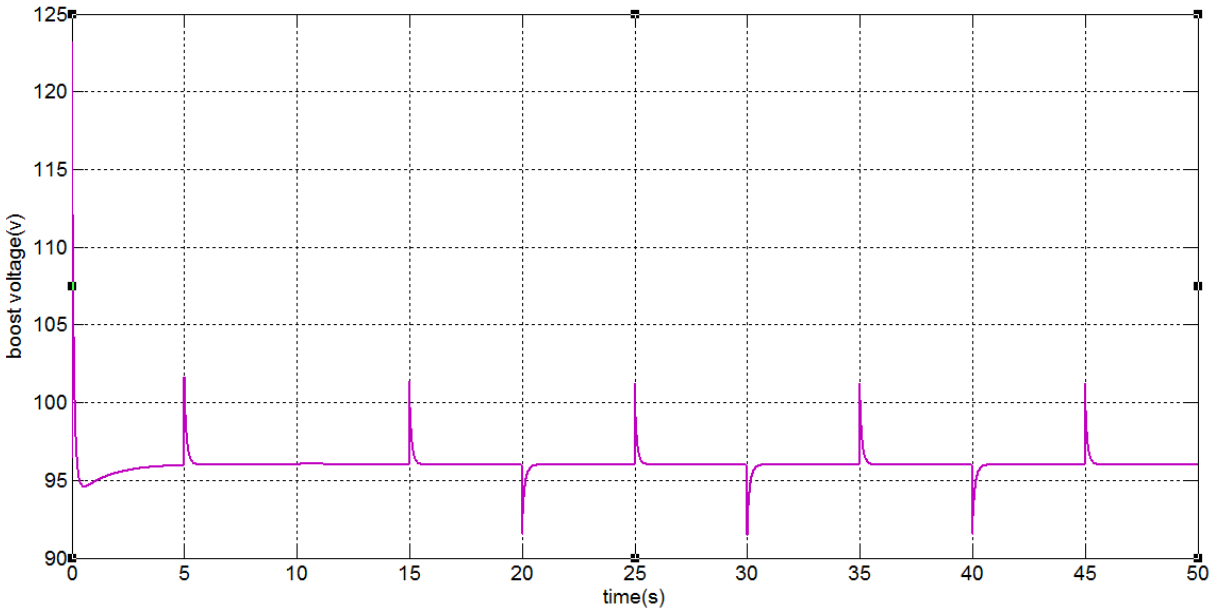

Graph 4.13 Boost output voltage versus time

At the switching instant of the load boost voltage has change for a very short time interval (shown in Graph 4.13**)**, this is what we were looking for.

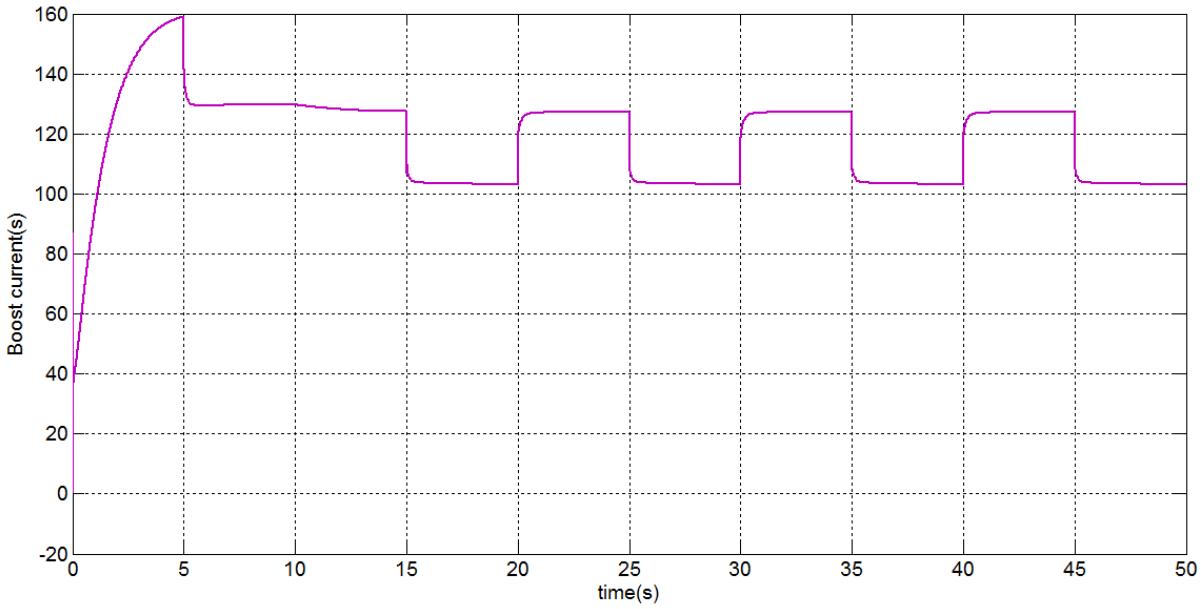

\

Graph 4.14 Boost output current versus time

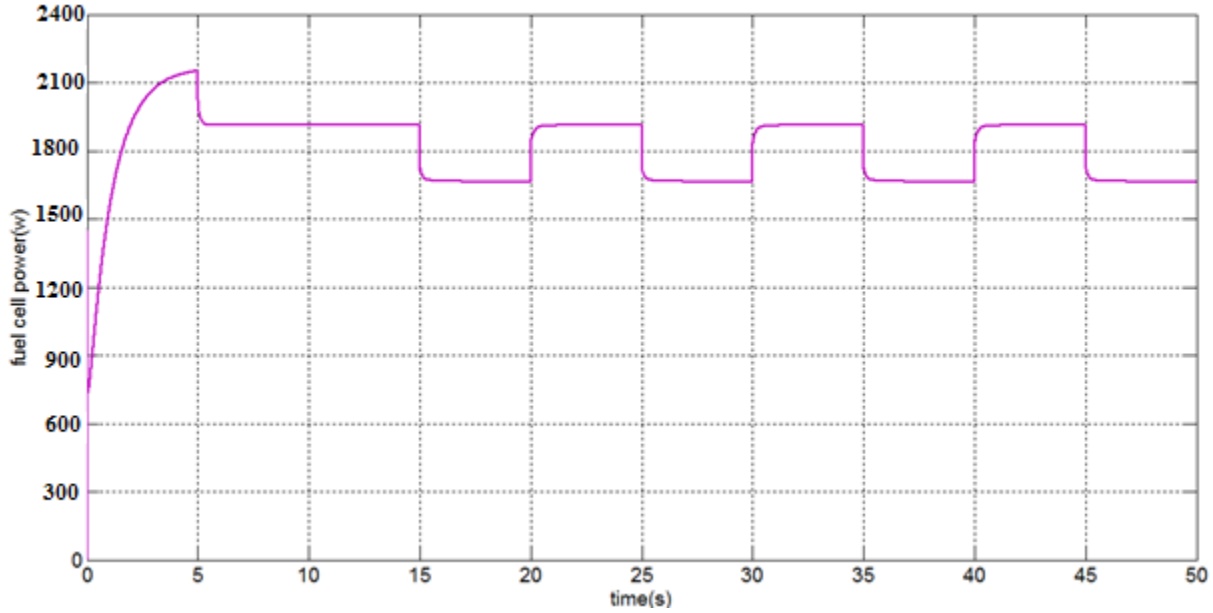

Graph 4.15 Output power of fuel cell versus time

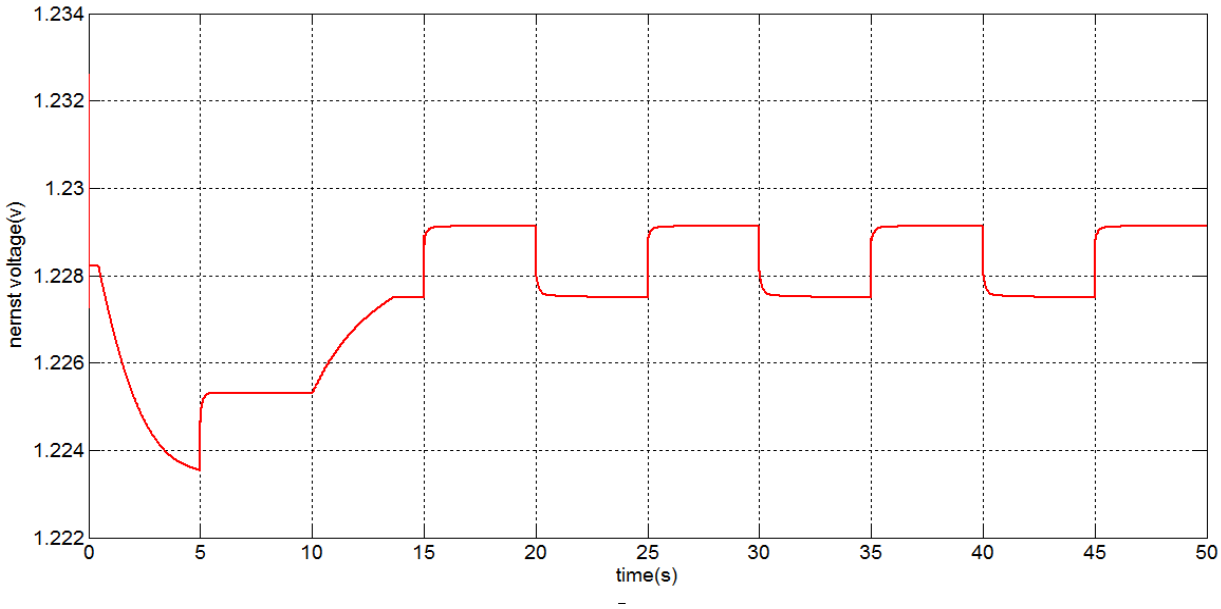

Graph 4.16 Nernst voltage versus time

4.4.2 Result Demonstration:

With the change in load, output current has changed. PI controller scale the error, caused by change in load, and the output voltage as shown in Graph (4.13) settled to the reference value in very short time interval (250 ms) .As output current changes with the change in load, the output power also changes from 2.4 kW to 2.1 kW. Current dependent thermodynamic potential (E_{Nernst}) as shown in Graph (4.16) is also changed. As the fuel cell voltage depends on Nernst voltage and other factors, so fuel cell voltage also changes with switching of load.

Summary:

Fuel cell system is an energy system, whose output voltage (v_fc) depends on so many parameters, which makes it complex system. Output voltage of this energy system will change with any of the parameter variation. Voltage of this system under the flow rate variation and load variation is very well regulated by the converter with a PI controller.

Chapter 5

Implementation of Fuel Cell System Using VHDL and Hardware Prototyping of (PI+PWM)

Chapter 5

Implementation of Fuel Cell System Using VHDL and hardware Prototyping of (PI+PWM)

5.1 Introduction:

The recent advancement of VLSI technology, strongly enabled by Electronic Design Automation (EDA) tools has created the opportunity for the development of complex and compact high performance controllers for power electronic systems [1]. This approach extends the use of high level digital language to make a high efficient controller for a complex electrical circuit. This has made possible due to the synthesis of the whole system in a single environment.

To achieve a high precision, floating type package of 32 bit (fphdl32_pkg) has added to the VHDL library.

Complex equations like logarithmic and exponential function has approximated by using its expansion series (Taylor series). We had applied differentiation and integration by numerical method (Euler Forward method) e.g. differentiation of y with respect to x is given by $\frac{dy}{dx} = \frac{y_{n+1} - y_n}{x_{n+1} - x_n}$.

Boost current has been discretized using the equation [18].

$$i(n+1) = \left(\frac{V_{fc} DT}{L} + i(n) - \frac{V_{fc}}{R} \right) e^{-\frac{R(1-D)T}{L}} + \frac{V_{fc}}{R} \qquad (5.1)$$

5.2 Implementation of Dynamic model of Fuel cell

We have seen in chapter 2, only three parameters, activation overvoltage, ohmic voltage and concentration overvoltage of dynamic model (electrochemical model) depends on the fuel cell current. In order to reasonably simplify the solution of dynamic model, we have taken two look up table, one for ohmic overvoltage, and other for activation overvoltage, as expression for concentration overvoltage is simple we have directly applied this by Taylor series expansion method. We have taken, such values in look-up tables, which can give better approximation after implying it through convolution linear curve fitting equation. In order to

simplifying the dynamic model, the partial pressure of hydrogen P_{H2} of the fuel cell system is normally kept constant, and the temperature is also kept constant. With these assumptions, the dynamic model of the fuel cell can be implemented in a simple way.

5.3 Converter part implementation

The boost converter, fuel cell and load are simulated with a sample time T_S = 100 μs. The controller is simulated with a higher sample time T_s = 10 ms, since the FCS's dominant time constant is much higher [1]. The main reason to take short sample time is to reduce errors confine distortion and strengthen the stability. We have taken resolution (maximum number of pulses that we can pack into a PWM period) of the PWM 100 and frequency of the PWM is set equal to controller sampling frequency. Generation of PWM has done with the counter based topology.

5.4 PWM implementation

PWM is a modulation technique that generates variable width pulses to represent the amplitude of an analog input signal.

Pulse width modulation (PWM) is a powerful technique for controlling analog circuits with a processor's digital outputs. PWM is employed in a wide variety of applications, ranging from measurement and communications to power control and conversion. Through the use of high resolution counter, the duty cycle is modulated to encode a particular analog signal.

PWM signals are typically created by using a clock at some multiple of the switching frequency with a counter [19].

In order to get less quantization error of the duty cycle we have taken resolution of the PWM 100. As more bits of resolution are added to the error sample, the digital system starts to approach a linear analog controller.

It is impossible to choose frequency small enough to give fast transient performance without destabilizing the feedback loop, so we have limit the frequency of the PWM equal to controller sampling frequency.

There are various methods to generate PWM; few of them are described here.

5.4.1 High frequency counter based PWM Generator

This architecture in Fig. 5.1 was proposed by E.Koutroulis , A.Dollas and K.Kalaitzakis in [19].

In this architecture there is a high speed N-bit free running counter, N-bit register and N-bit comparator. Output, coming from counter is used to be compared with register output, which stores desired input duty cycle (N-bit value), with the help of comparator. The comparator output is set equal to "1" when both counter and register output values are equal. This comparator output is used to set RS latch. The overflow signal gets high when counter reach to its maximum value. This overflow signal is used to reset RS latch, and to load new input data in register. The output of RS latch gives the PWM output. It can be used to generate High-frequency PWM output which is not possible in normal counter based approach.

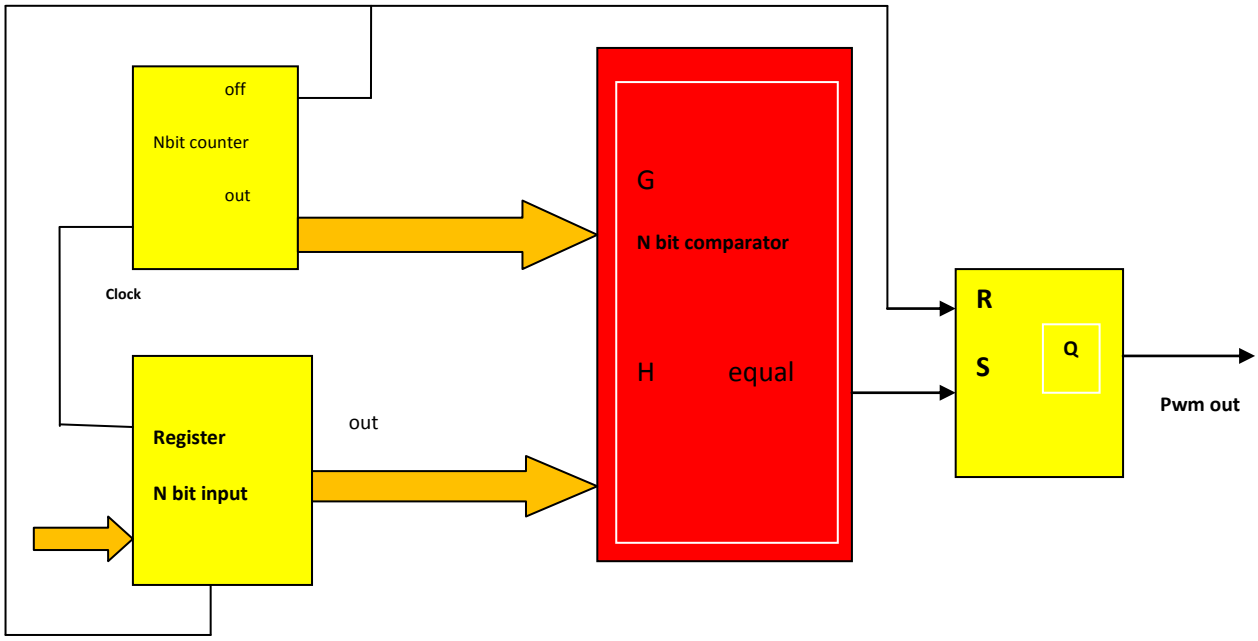

Fig.5.1 Architecture of PWM Generator proposed by E. Koutroulis

5.4.2 Counter based PWM Generator

In digital systems, PWM signals are typically created by using a clock at some multiple of the switching frequency with a counter. The PWM signal is set high at the beginning of a switching period and then reset after the counter detects that some number of cycles of the faster clock have passed [20].

Counter clock frequency in this architecture is chosen to be 2^N times of the switching frequency of the converter, where N is the number of bits. This architecture is well suited for ultrafast clocked-counters. Architecture of this type of digital PWM generator is depicted as below in the Fig.5.2. This is acceptable for dc–dc converters that deliver power in the watt range, but not for systems in the milli watt range.

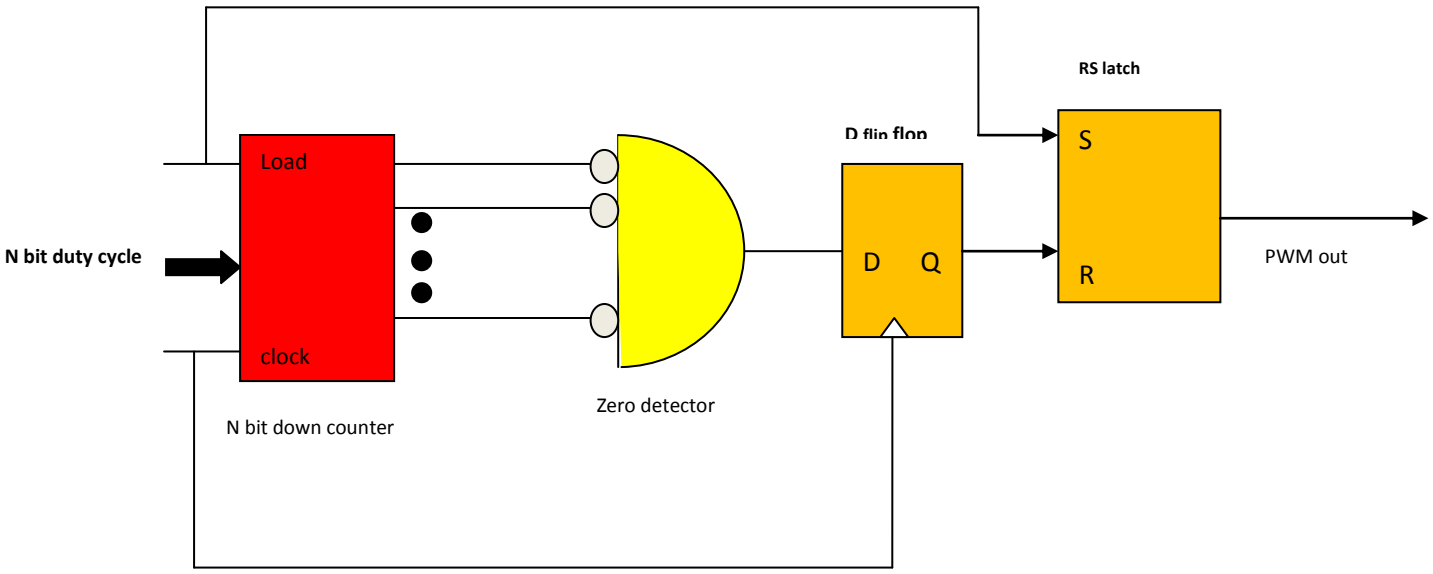

Fig.5.2 Architecture of Counter based PWM Generator proposed by A.P Dancy.

5.4.3 Cascaded Counter based PWM generator

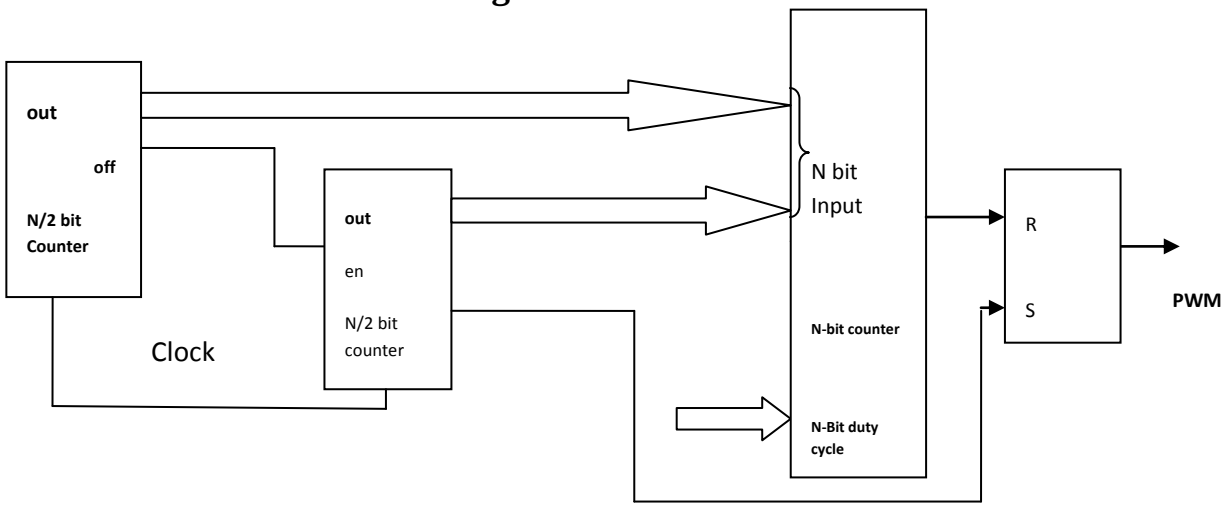

Fig.5.3 Cascade counter based PWM generator

In this architecture shown in Fig.5.3**,** two N/2 bit counters are cascaded together. In order to compare the output data of both counters is given to the N-bit input of comparator, where these data get compare with duty cycle. The output of comparator is "1" when both value matches together. This comparator output is used to reset the RS latch. MSB counter overflow signal is used to set RS latch, whenever it becomes activated by overflow of the LSB counter value. The PWM output is given by RS latch.

5.4.4 Proposed method

In this method up counter is used. The value generated by this up counter is compared by the data, with the help of a comparator. PWM has set to value‘1’ if the input data is less than the value of the current count of the counter, and it has set to’0’,when the input data is greater than count value. Period of PWM can be set with the help of maximum count of the up counter.RTL schematic of this method is shown in Fig.5.7

RTL schematic of the different methods discussed above:

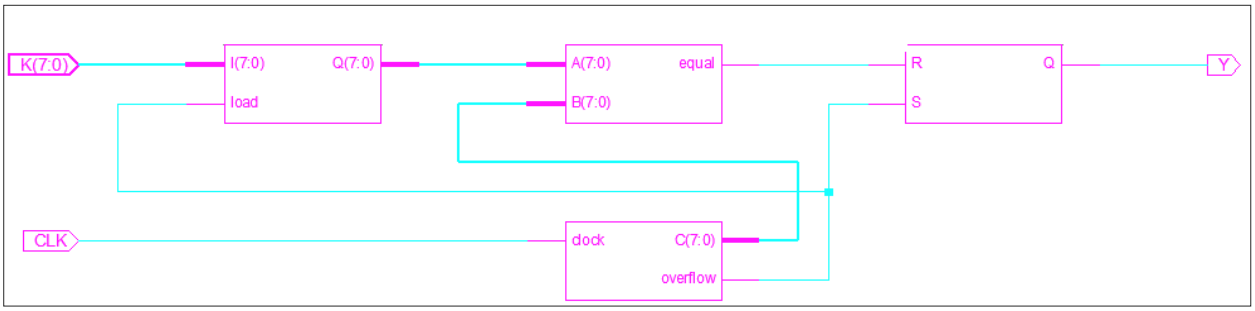

Fig.5.4 RTL Schematic of high frequency based PWM generator

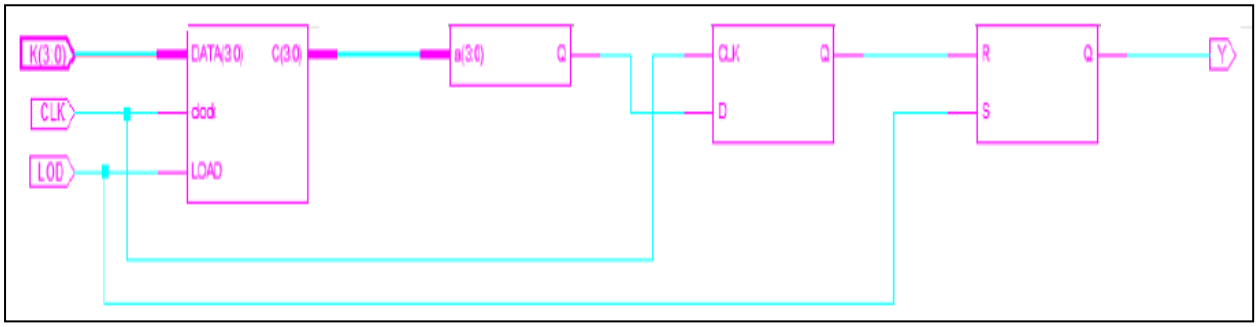

Fig.5.5 RTL Schematic of counter based PWM generator

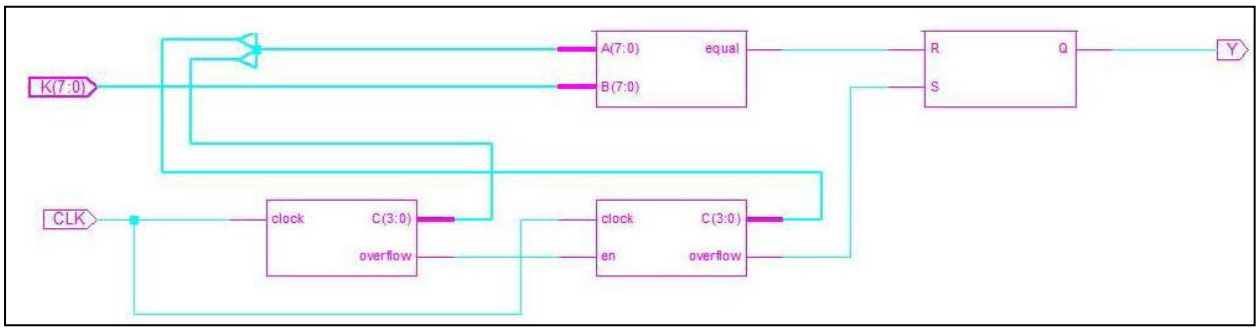

Fig.5.6 RTL schematic of cascaded counter based PWM generator

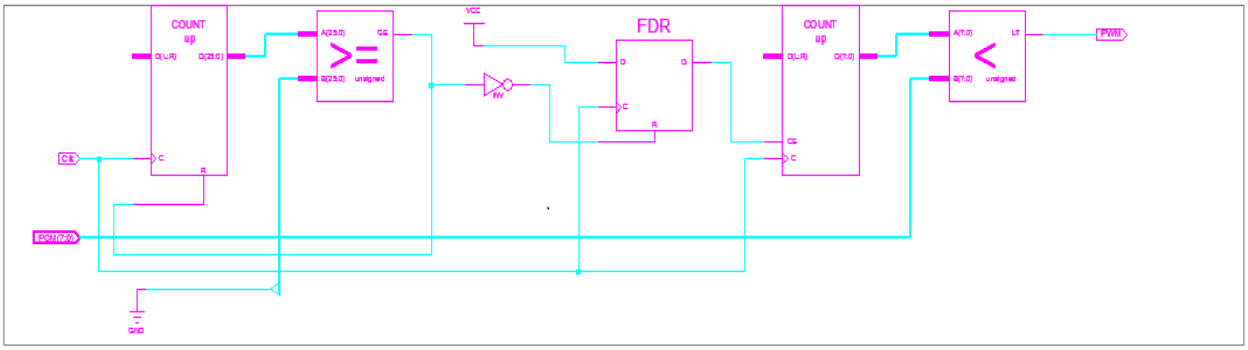

Fig.5.7 RTL schematic of method discussed in 5.4.4

Theoretical value of duty cycle is given by the relation:

$$D = \frac{Integer\ value\ of\ \ N\ \ Bit\ \ data}{2^N} \qquad (5.2)$$

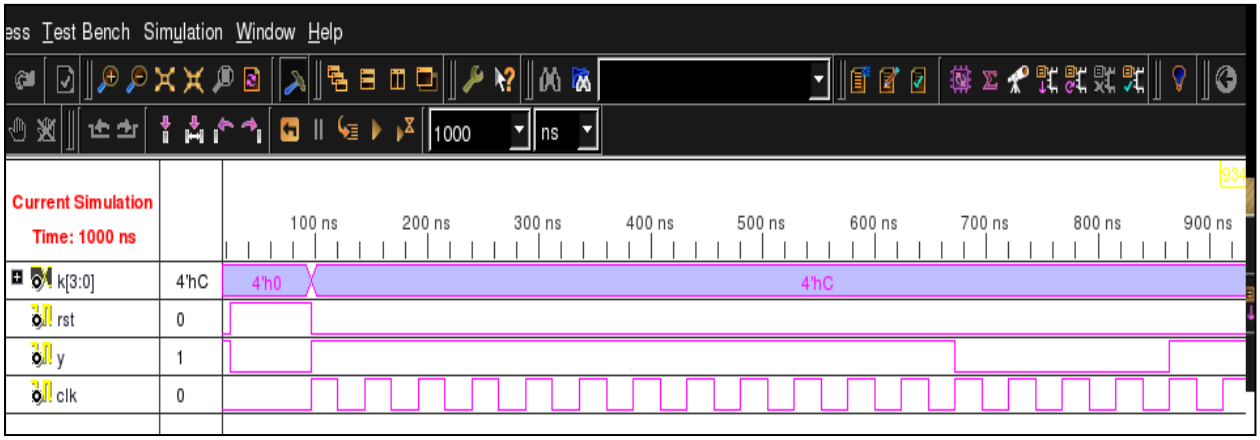

Fig.5.8 Test Bench waveform of PWM generator

K = "1100"

Duty cycle =12/16=0.75 (from equation 5.2)

From Test Bench waveform D= 670-100/760 =.75

We have got the same value of D as theoretical value of it.

5.5 PI implementation

PI controller is used to control the duty cycle of varying error signal due to variation in load, which in turns set the output voltage to reference voltage in very short time. Discretization of this PI controller has done through the discrete equation:

$u(n+1) = k_1\, u(n) + k_2 e(n-1)$.

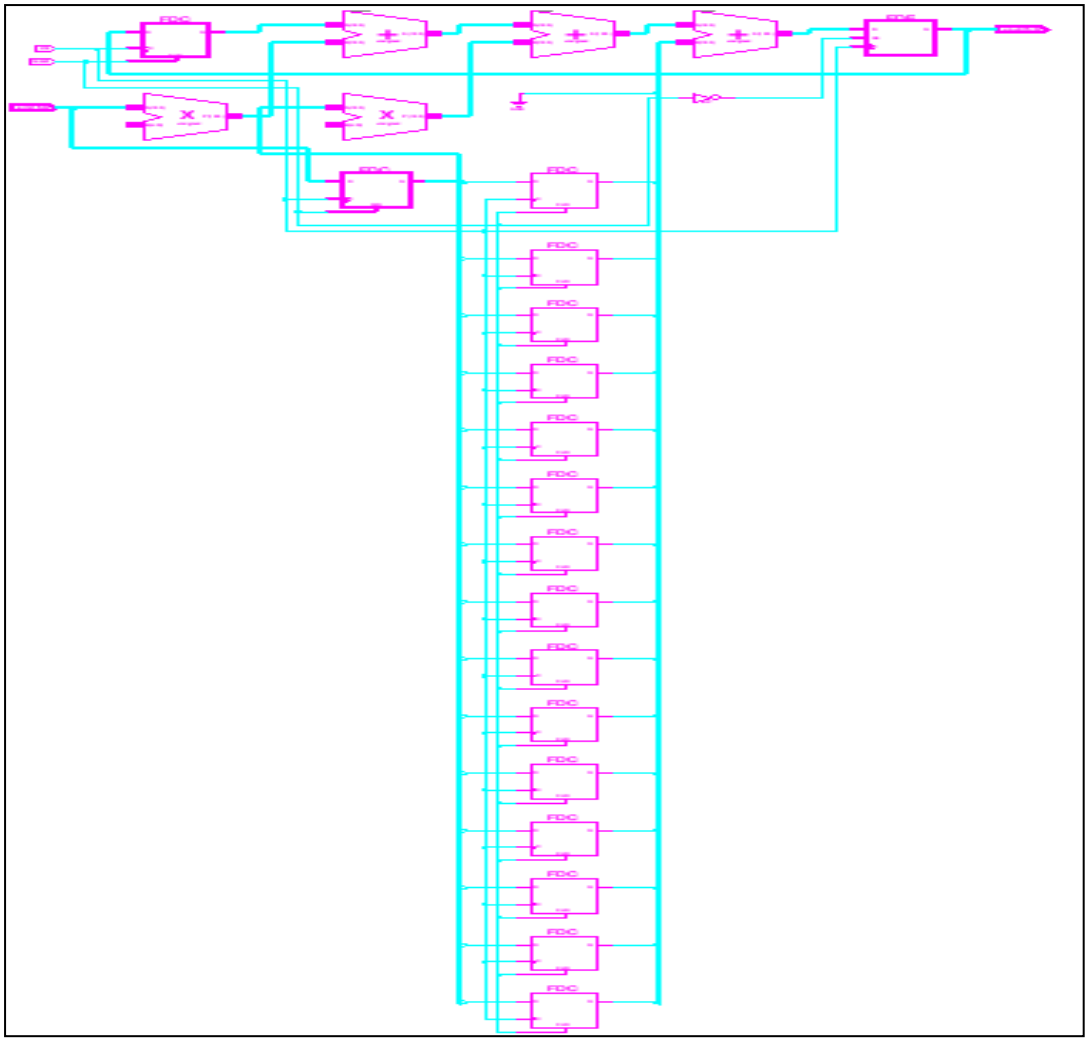

Fig.5.9 RTL Schematic of PI Controller

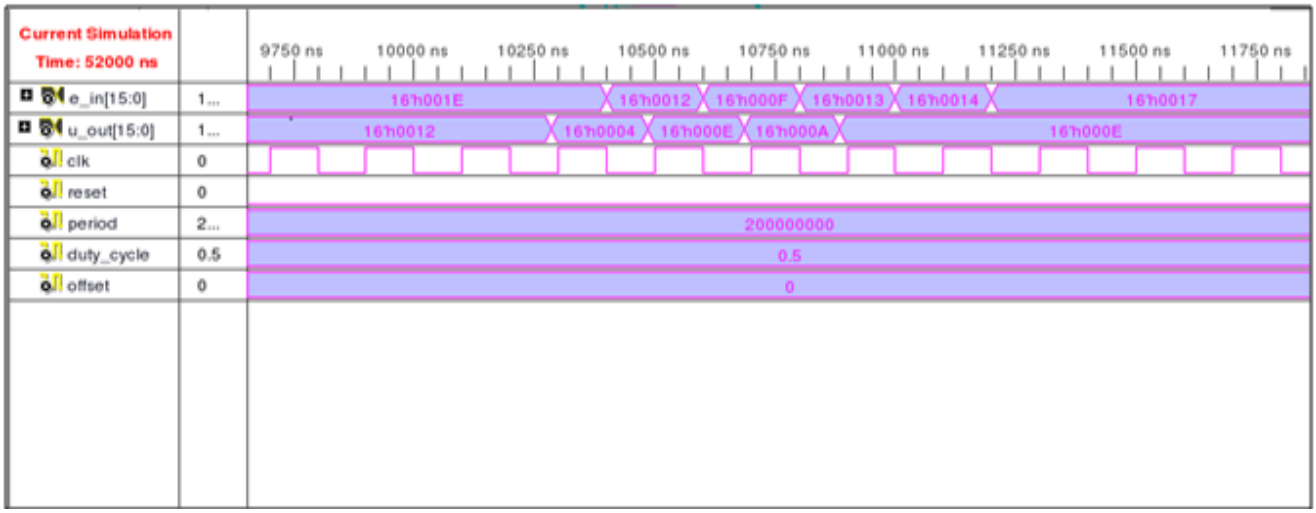

Fig.5.10 Test Bench waveform of PI controller

We can see in the above Test Bench waveform, that error signal at time 10500 ns, e_in has a value of 12 H and its corresponding output has a value of 4 H, which is less compare to e_in. On the basis of above study of Test Bench waveform we can say that the error signal has got scaled by the PI controller. We can use this PI controller to scale the duty cycle of the PWM, so that the PWM waveform cannot change for a little variation of error signal, and thus we can get constant output voltage with a little change in load value.

5.6 State Diagram of Fuel Cell System for VHDL Implementation

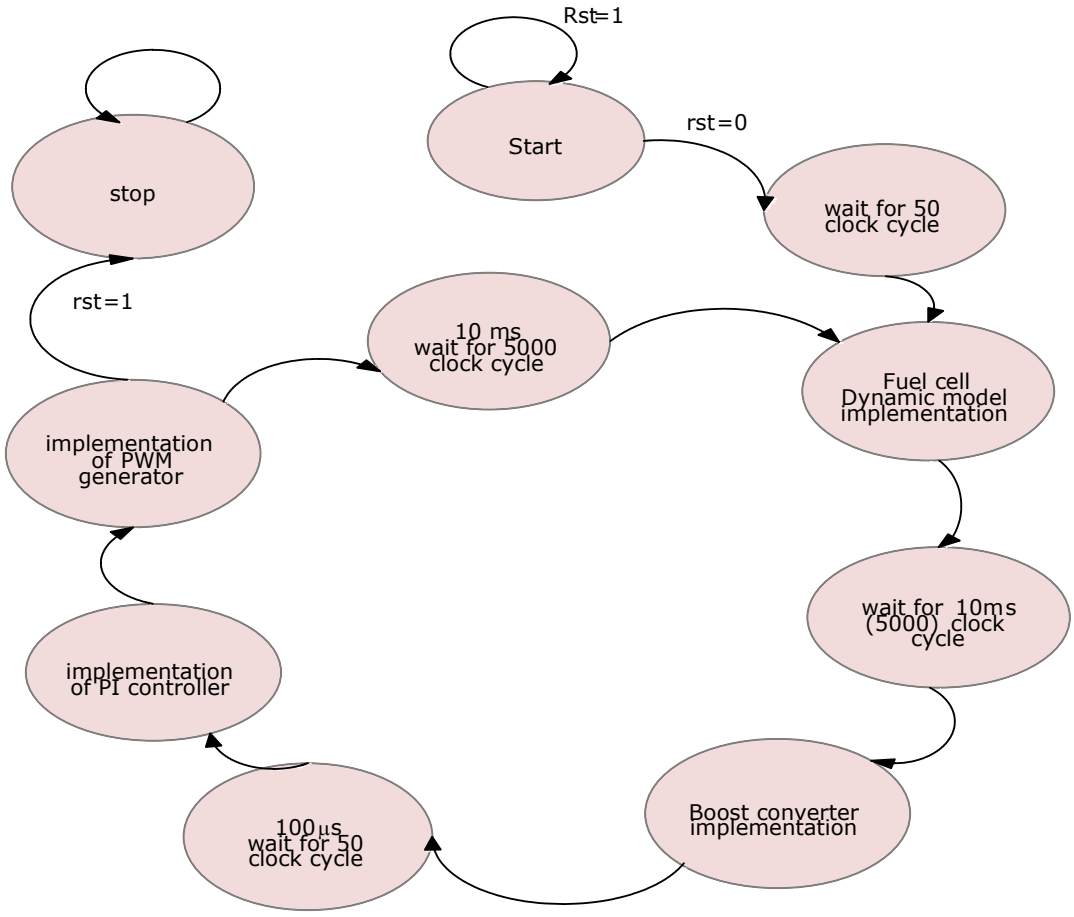

In order to create delay for sample time, we have taken counter. As we know that, the onboard clock cycle frequency is 50 MHz, which is equal to a time period of 20 ns. In order to create 10 ms delay between two samples of converter we have taken 5000 clock cycle, and in order to create 100 µs delay for PWM we have taken 50 clock cycles.

5.7 Result and Discussion

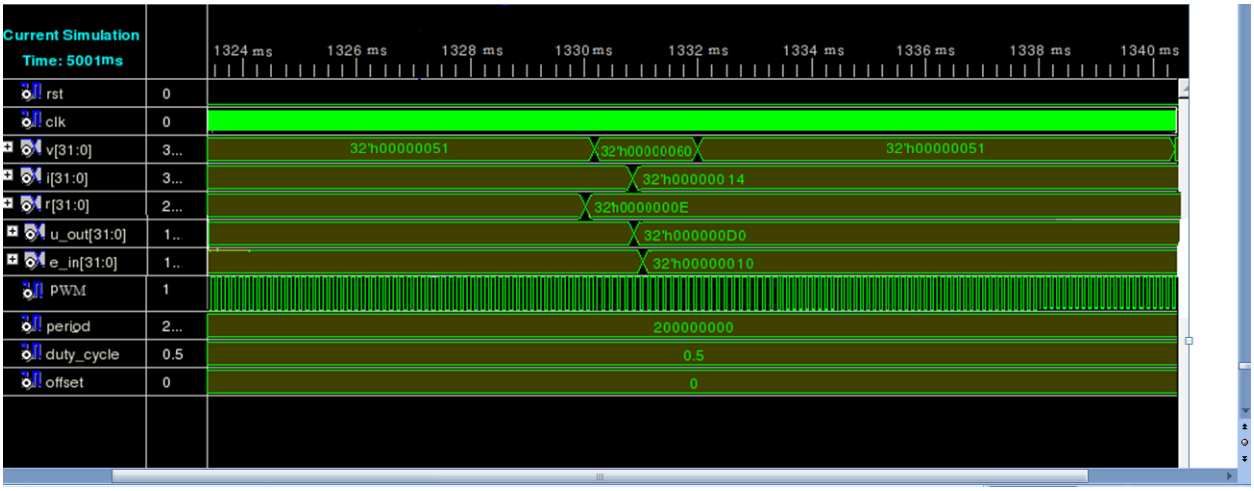

Fig.5.11 Test Bench Waveform OF The Fuel Cell System Using XILINX ISE Simulator

In the above Test Bench when the resistance has changed, current and voltage has also changed, but voltage settled to its previous value after a short time. In the above test bench waveform u_out and e_in are output and input of the PI controller respectively. We can see that the error signal e_in got scaled with the help of PI controller. Duty Cycle of PWM got changed due to change in the error signal. For above simulation we have taken simple hexadecimal value instead of floating point data, we can take floating point data for a better precision.

5.8 Real Time Debugging of the Fuel Cell System

After doing Placement and Routing, the VHDL code of fuel cell power system was downloaded into the SPARTAN3E FPGA board and Real time debugging was done for the fuel cell system. The clock for the architecture was provided by clock (C9) present in FPGA board, reset input has applied to K18 pin of the SPARTA3E board, Controller output has applied to a led (F9). At first, we have analyzed the output of controller with the software Chip Scope Pro Analyzer, and then by using CRO we have seen the PWM output of controller. In order to see the waveform on CRO we have assigned an output pin on FPGA board.

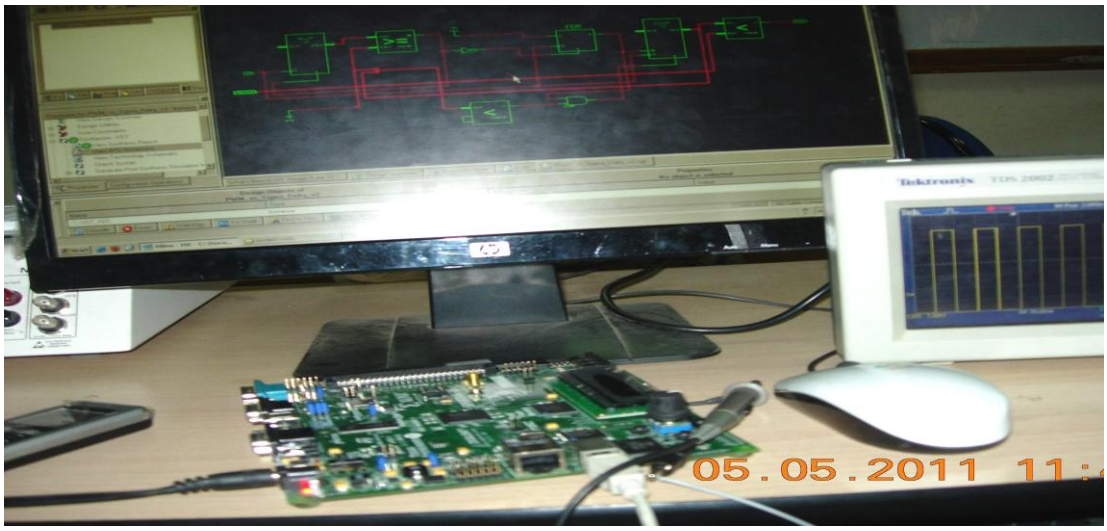

Fig.5.12 Experimental setup

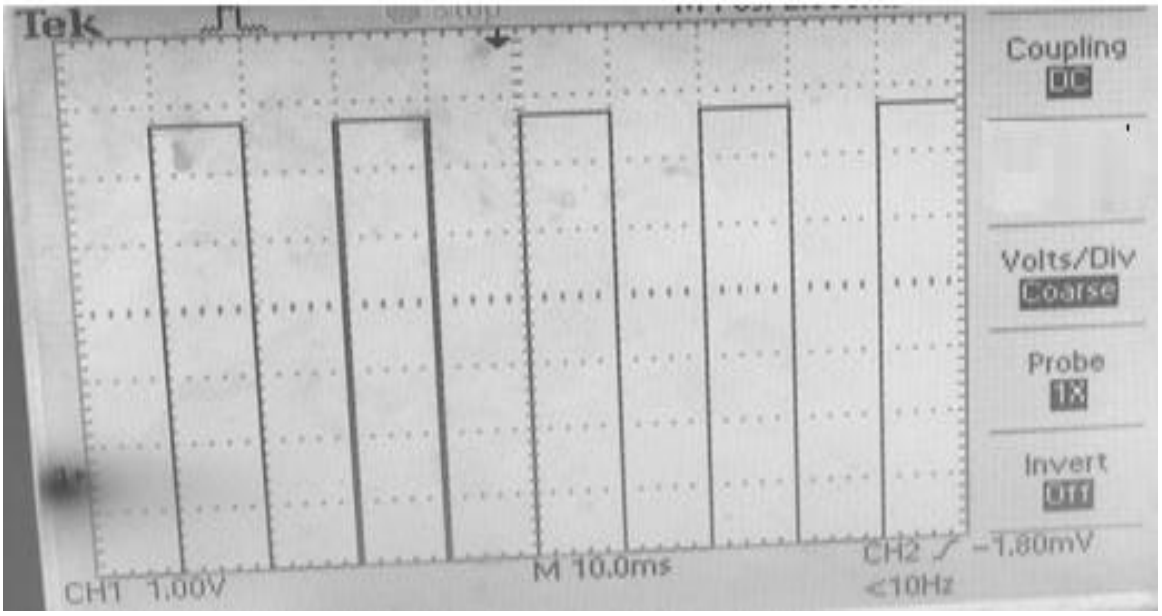

Fig.5.13 Resulted PWM with Duty cycle D =.5 at the output pin of the SPARTAN3E with oscilloscope

Waveform of PWM, which is shown above is having a duty cycle of 0.5 and frequency of 100 kHz, that is what we require to convert a 48 v dc to 96 v dc, with the help of a Boost-Converter.

Chapter 6

Conclusions and future work

Chapter 6

Conclusion and Future Work

6.1 Conclusion:

In order to examine the possibility to implement digital controller based on FPGA prototyping, a new method is proposed and analyzed. The proposed digital controller is able to control the output of any renewable energy sources. A method to synthesized whole fuel cell power system is developed using VHDL. This approach using VHDL is applied to a fuel cell power system of 2.4 kW and 96 v is. The proposed method is simulated, and the results demonstrate appropriate performance of the system and controllers. This thesis presents a very simple and reasonable approach to model a particular PEM (Polymer electrolyte membrane) fuel cell, and its real time debugging using SPARTAN3E board. Initially the system were simulated in Matlab/Simulink, to make a reference for VHDL implementation, after the Matlab/Simulink modeling, fuel cell system model has developed in VHDL by using some approximation and assumption. The work carried out in this thesis has allowed to prototype hardware of fuel cell controller.

6.2 Future Work:

This prototyped board controller can be used with a real fuel cell. The novel approach proposed in this thesis can be also used with another type of renewable sources.

.

References:

[1] K. Petrinec, M. Cirstea, , K. Seare, C. Marinescu "A Novel FPGA Fuel Cell System Controller Design".11th International conference on Optimization of Electrical and Electronic Equipmen,2008, pp. 401-406.

[2] Nehrir.H, Caisheng Wang, Shaw, S.R, 2006. "Fuel cells: promising devices for distributed generation", *IEEE Power and Energy Magazine*, vol. 4, issue 1, pp. 47-53.

.

[3] K. Petrinec, M. Cirstea, "Holistic modelling of a fuel cell power system and FPGA controller using Handel-C", *IEEE IECON'06*, Paris, France, November 7-10, 2006.

[4] *http://vega.unitbv.ro/~ieee*

[5] Rahim N.A. and Islam Z., "Field Programmable Gate Array-Based Pulse-Width Modulation for Single Phase Active Power Filter"; American Journal of Applied Sciences, Vol.6 (2009): pp. 1742-1747.

[6] ElieLafy,Marie-Cecile pera and Daniel hissel femto "PEM fuel cell modeling with static dynamic decomposition and voltage rebuilding" *IEEE Transaction* on Power Electronics, vol.19, issue 5,Sept 2004, pp-1234 – 1241.

[7] J. Larminie and A. Dicks: Fuel Cell Systems Explained. 2nd ed, J. Wiley & Sons, England, 200**3.**

[8] G. Kortum, Treatise on Electrochemistry (2nd Edition). New York: Elsevier, 1965

[9] J. C. Amphlett, R. M. Baumert, R. F. Mann, B. A. Peppley, and P. R. Roberge, "Performance modeling of the Ballard Mark IV solid polymer"

[10] M.T. Iqbal, "Modeling and control of a wind fuel cell hybrid energy system", Renewable Energy, vol. 28, issue 2, Feb. 2003, pp. 223 – 237. electrolyte fuel cell, I. Mechanistic model development," *J. Electrochem. Soc.*, vol. 142, no. 1, Jan. 1995, pp. 1–8.

[11] J.M. Correa, F.A. Farret, L.N. Canha, M.G. Simoes, "An electrochemical-based fuel-cell model suitable for electrical engineering automation approach," *IEEE Trans*. Ind. Electronics, vol. 51, issue 5, Oct. 2004, pp.1103 – 1112.

[12] R.F. Mann, J.C. Amphlett, M.A.I. Hooper, H.M. Jensen, B.A. Peppley, P.R. Roberge, "Development and application of a generalised steady-state electrochemical model for a PEM fuel cell," *Journal of Power Sources*, vol. 86, issues 1-2, Mar. 2000, pp. 173 – 180.

[13] Fuel Cell Handbook (Fifth Edition), EG&G Services, Parsons Inc., DEO of Fossil Energy, National Energy Technology Lab, Oct. 2000. *IEEE Transactions* on energy conversion, vol. 20, no. 2, June 2005.

[14] CaishengWang, ,M. Hashem Nehrir, and Steven R. Shaw, "Dynamic Models and Model Validation for PEM Fuel Cells Using Electrical Circuits" *IEEE Transaction* on Energy conservation,vol.20, issue 2, June 2005, pp.442-451.

[15] A. Schneuwly,M. Bärtschi, V. Hermann, G. Sartorelli, R. Gallay, and R. Koetz, "BOOST CAP double-layer capacitors for peak power automotive applications," in Proc. 2nd Int. Advanced Automotive Battery Conf., Las Vegas, NV, Feb. 2002.

[16] *http://en.wikipedia.org/wiki/Buck_converter*

[17] *http://en.wikipedia.org/wiki/Boost_converter*

[18] Ataollah Abbasi Mehrdad rostami Jafar abdollahi and Hamid abbasi hasan.n "An analytical discrete model for evaluation the chaotic behavior of Boost converter under current control mode" Symposium on Industrial Electronics and Applications (ISIEA 2009), October 4-6, 2009, pp.-403-407.

[19] Koutroulis E., Dollas A. and Kalaitzakis K., "High-frequency pulse width modulation implementation using FPGA and CPLD ICs", Journal of Systems Architecture , Vol.52 (2006): pp. 332–344 .

[20] Dancy A.P., Amirtharajah R. and Chandrakasan A.P., "High-Efficiency Multiple-Output DC–DC Conversion for Low-Voltage Systems", *IEEE Trans*. on Very Large Scale Integration (VLSI) Systems, Vol. 8, No. 3, June 2000: pp.252-263.